SYNTHESIS AND REALIZATION OF CRYSTAL FILTERS

DAVID I. KOSOWSKY

TECHNICAL REPORT 298

JUNE 1, 1955

RESEARCH LABORATORY OF ELECTRONICS
MASSACHUSETTS INSTITUTE OF TECHNOLOGY
CAMBRIDGE, MASSACHUSETTS

The Research Laboratory of Electronics is an interdepartmental laboratory of the Department of Electrical Engineering and the Department of Physics.

The research reported in this document was made possible in part by support extended the Massachusetts Institute of Technology, Research Laboratory of Electronics, jointly by the Army (Signal Corps), the Navy (Office of Naval Research), and the Air Force (Office of Scientific Research, Air Research and Development Command), under Signal Corps Contract DA36-039 sc-42607, Project 102B; Department of the Army Project 3-99-10-022.

MASSACHUSETTS INSTITUTE OF TECHNOLOGY
RESEARCH LABORATORY OF ELECTRONICS

Technical Report 298 June 1, 1955

SYNTHESIS AND REALIZATION OF CRYSTAL FILTERS

David I. Kosowsky

This report is based on a thesis submitted to the Department of Electrical Engineering, M.I.T., June 1955, in partial fulfillment of the requirements for the degree of Doctor of Science.

Abstract

A new technique has been developed for the synthesis and realization of bandpass filters employing quartz resonators. By the use of approximation methods, crystal filter design is simplified to the point at which synthesis may be accomplished with only a slide rule and a number of plotted curves. The problem of obtaining piezoelectric resonators adjusted to extremely close tolerance was solved by the development of a new crystal-measuring procedure. Several crystal filters were constructed, and an excellent correspondence was found between calculated and measured characteristics.

I. PIEZOELECTRIC MATERIALS

1.1 INTRODUCTION

A piezoelectric material is one in which an electric stress applied in the direction of a specific crystallographic axis gives rise to a proportional mechanical stress along a related axis, and vice versa. The existence of the piezoelectric effect in quartz and other materials was discovered by Pierre and Paul-Jacques Curie and was announced in 1880.

The first practical application of the piezoelectric effect grew out of an experimental program started in 1915 by Paul Langevin at the request of the French Navy Department to devise a means of detecting submarines. Langevin's device was not perfected until the end of World War I but it found ready use as a sonic depth finder.

At about the same time, A. M. Nicolson, of Bell Telephone Laboratories, working with piezoelectric Rochelle salt, and Walter G. Cady, of Wesleyan University, working with quartz, showed that these materials could be successfully employed in oscillator circuits. The subsequent development of low temperature-coefficient quartz resonators made possible the stable piezoelectric crystal oscillator.

In 1922, Cady (2) proposed the use of a crystal as a frequency selective element by taking advantage of the sharp maximum in current through the crystal at its resonant frequency. The combination of crystals, inductances, and capacitors in lattice networks by Warren P. Mason (4, 5) made possible the many contemporary applications of crystal filters.

Because of the very low dissipation inherent in the quartz resonator, it is possible to make filters with very high selectivity. Crystal filters are used in noise and sound analyzing devices which permit frequency spectra to be obtained with very high resolution; in carrier systems for separating out control frequencies; and in radio communication systems for selecting harmonics of local oscillator signals. They have also been applied to carrier telephone systems (6) requiring very small channel spacings; to single sideband systems for separating the two sidebands; and to amplifiers in which very high selectivity is desired.

1.2 THE QUARTZ RESONATOR AND ITS EQUIVALENT CIRCUIT

Of the hundreds of crystals that exhibit the piezoelectric effect, only the quartz crystal has been employed to any significant extent in oscillators and filters. Any plate cut from a piece of natural quartz has a number of resonant frequencies that depend on the crystal dimensions, the vibrational mode involved, and the orientation of the cut. In the vicinity of a resonant frequency, the crystal can be replaced by an equivalent electric circuit (3, 9) of the type shown in Fig. 1a. The inductance L_1 and capacitance C_1 represent the effective mass and stiffness of the crystal, respectively. C_o is the static capacitance that would be measured if he crystal were not vibrating. The resistance

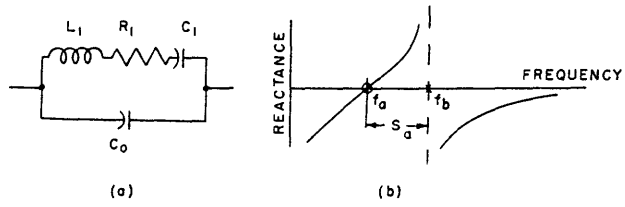

Fig. 1. Equivalent circuit of crystal resonator.

R_1 represents the frictional loss of the vibrating crystal. The ratio of the reactance of L_1 at the resonant frequency to the resistance R_1 (crystal Q) is generally of the order of 20,000 when the resonator is mounted in air, but when the units are carefully mounted in vacuum, it may be (10) of the order of 500,000. Because of this extremely low dissipation, the crystal may be considered a purely reactive network for most filter applications.

The reactance curve corresponding to the resonator equivalent circuit is shown in Fig. 1b. The resonant frequency or zero of the crystal unit (f_a) and the antiresonant frequency or pole (f_b) are related to one another by the ratio of capacitances of the crystal defined by

$$r = \frac{C_o}{C_1} \tag{1}$$

The relationship is easily seen to be:

$$f_b^2 = f_a^2\left(1 + \frac{1}{r}\right) \tag{2}$$

Because of the coupling that exists between the electrical and mechanical stresses within the crystal, there will always be a fixed ratio of capacitances for any crystal cut (1). The lowest ratio found for quartz is 115 but, because of stray-wiring capacitance and crystal-holder capacitance, the minimum ratio (r_x) for practical quartz cuts is approximately 125. From Eq. 2, the zero-pole spacing (S_a in Fig. 1b) can be approximated by

$$S_a = f_b - f_a \approx \frac{f_a}{2r} \tag{3}$$

If capacitance is added in series or in parallel with a crystal unit, r will increase and, correspondingly, S_a will decrease. It will become evident later that bandpass filters employing only crystals and capacitors as elements will have bandwidths that can be no greater than twice the zero-pole spacing of a crystal-capacitor combination. Therefore, capacitance added in any manner to a crystal can only reduce the filter bandwidth. In Section III, a method is described for producing wideband crystal filters by employing inductances in series or in parallel with crystal units. In the final analysis,

however, the bandwidth of narrow- or wide-band crystal filters will be limited to a maximum value determined by the criterion

$$r \geqslant r_x \tag{4}$$

where r is the smallest ratio of capacitance required by the crystal elements in the filter, and r_x depends on the crystal cut employed, but it will rarely be smaller than 125 for any quartz resonator.

In addition to the fixed ratio of capacitances which is characteristic of any crystal cut, the value of an electrical parameter, such as the crystal inductance (L_1), is limited to a narrow range by such factors as resonant frequency, mechanical stability, temperature coefficient, and suppression of spurious modes of vibration. In the crystal filter, this limitation appears as a corresponding restriction on the realizable image-impedance range, and in wideband filters it may further limit the range of realizable bandwidths.

Detailed data relative to the quartz-crystal cuts commonly employed in filters, together with the frequency and inductance constants necessary to dimension the resonators, will be found in references 2, 11, 14, and 38. In general, the equivalent inductance of a crystal will be considerably greater in value than any lumped inductance that can be realized at the resonant frequency of the crystal. For example, at 100 kc/sec, typical crystal inductances range from 10 to 100 henries.

1.3 DIVIDED-PLATE CRYSTAL UNITS

To prepare a crystal resonator for use in a filter circuit, it is desirable to deposit a thin film of conducting material on the major faces of the crystal. Electric contact is made to the plating by means of conducting wires, which are soldered to the plate. These wires, which also provide mechanical support for the crystal, as shown in Fig. 2a, are mounted at points on the crystal plate which are nodes of motion for the resonator (11). In this manner, the restraining force exerted by the support wires has little effect upon the vibration of the crystal.

Crystal filters are very often realized in the form of a symmetrical lattice network employing one or more crystals in each lattice arm. Since the symmetrical lattice requires elements in identical pairs, quartz resonators are often fabricated with divided platings (16), as shown in Fig. 2b. The divided-plate crystal is a four-terminal symmetrical network that can be represented in balanced lattice form. Depending on how the input and output terminals are chosen, the equivalent lattice will have a crystal in either the series or shunt arms of the lattice (17). One choice of terminals is shown in Fig. 2c; the impedance of the crystal in the series arm of the lattice is twice that of the fully plated crystal. The capacitors C_{13} and C_{14} represent stray capacitances between terminals 1-3 and terminals 1-4, respectively. Bandpass lattice filters generally make use of crystals in both series and shunt arms, in which case the divided-plate connections shown in Fig. 3a are employed. The subscripts A and B define

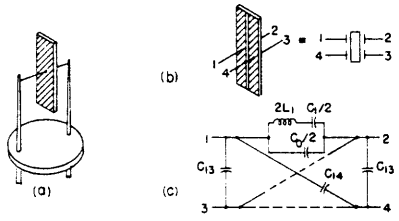

Fig. 2. Plated crystal resonators.

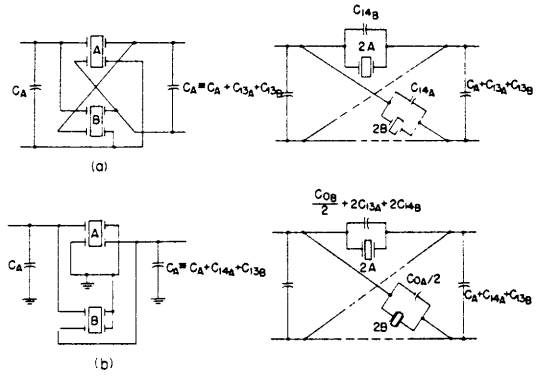

Fig. 3. Divided-plate crystal connections: (a) balanced; (b) unbalanced.

elements of crystals A and B, respectively. Crystals 2A and 2B have twice the impedance of A and B, respectively.

If an unbalanced filter is desirable, the divided-plate connections of Fig. 3b may be used. Note, however, that half the static capacitance (C_o) of each crystal appears in parallel with the other. In effect, the ratio of capacitances of the resonators is thereby doubled, and the realizable bandwidth is correspondingly decreased. In addition, a restriction on the attenuation characteristic results from the presence of $2C_{13A} + 2C_{14B}$ in the series arm of the lattice. This capacitance, which is not balanced by capacitance in the shunt arm, will cause the attenuation peaks of the filter to lie very close to the passband, and special plating methods must be employed to obtain reasonable attenuation characteristics (17).

II. THE SYMMETRICAL LATTICE FILTER

2.1 IMAGE PARAMETERS

The symmetrical lattice or bridge, which is the most general form of symmetrical network (18), is particularly well suited to crystal-filter design. In addition to the advantage of analytical flexibility offered by the lattice network, practical considerations peculiar to crystal-filter realization often make it necessary to employ this structure to obtain desirable filter characteristics (4).

For the symmetrical lattice network, shown in Fig. 4, the image parameters (19) are very simple functions of the series and shunt impedances, Z_a and Z_b (18).

$$Z_o = (Z_a Z_b)^{1/2} \tag{5}$$

$$\tanh\left(\frac{\theta}{2}\right) = \left(\frac{Z_a}{Z_b}\right)^{1/2} \tag{6}$$

where Z_o is the image impedance, and θ is the image propagation constant. If a quantity p is defined by

$$p \equiv \left(\frac{Z_a}{Z_b}\right)^{1/2} \tag{7}$$

then Eq. 6 may be written in the equivalent form

$$\theta = \ln \frac{1 + p}{1 - p} \tag{8}$$

It follows that the attenuation loss, which is the real part of θ, is given by

$$\alpha = \ln \left|\frac{1 + p}{1 - p}\right| \tag{9}$$

If Z_a and Z_b are assumed to be pure reactances, the conditions under which the symmetrical lattice acts as a filter may be readily determined in terms of the signs of Z_a and Z_b. When the reactances Z_a and Z_b have opposite signs the value of Z_o given by Eq. 5 is real, and the value of p defined in Eq. 7 is imaginary. From Eq. 9, the attenuation is zero, and a passband is obtained. Similarly, the lattice filter has an attenuating- or stop-band whenever Z_a and Z_b have the same sign. Under these conditions, the image impedance is reactive and the attenuation becomes infinite whenever $p = 1$, or $Z_a = Z_b$.

An important property of the lattice filter is that the image impedance depends only on the number and location of the critical frequencies that are present in the stopband of the filter and upon the cutoff frequencies, while the attenuation (and phase in the passband) depends only upon the number and location of the critical frequencies that appear in the passband and upon the cutoff frequencies. It is therefore possible to

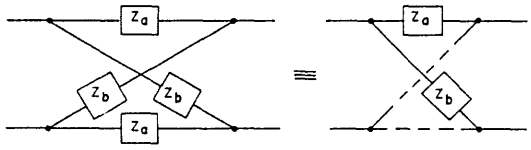

Fig. 4. Symmetrical lattice network.

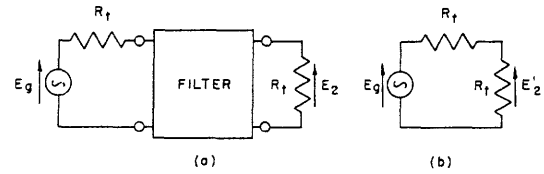

Fig. 5. Circuit for determination of insertion loss.

specify the image impedance and the attenuation of a lattice filter independently of one another, by suitable arrangement of the critical frequencies in the filter pass- and stop-bands.

2.2 INSERTION LOSS

The attenuation α of a symmetrical network expresses the loss introduced by the network when it is terminated in its image impedance. In practice, the terminal impedances of a filter are generally fixed resistances, so that the attenuation loss only approximately describes the performance of the filter.

The effect of placing a filter network between source and load resistances R_t, as shown in Fig. 5a, may be conveniently described in terms of the insertion loss it introduces. Accordingly, an insertion ratio is defined as E_2'/E_2 in Fig. 5b; that is, the ratio of the output voltage when the filter is not present (Fig. 5b) to the output voltage that results when the filter is placed between the resistances R_t (Fig. 5a).

If we define the normalized image impedance z_o by

$$z_o = \frac{Z_o}{R_t} \tag{10}$$

and the reflection coefficient ρ by

$$\rho = \frac{1 - z_o}{1 + z_o} \tag{11}$$

it can be shown (21) that the insertion ratio becomes

$$\frac{E_2'}{E_2} = e^{\theta}(1 - \rho^2)^{-1}\,(1 - \rho^2\, e^{-2\theta}) \tag{12}$$

The insertion loss α_N is the logarithm of the magnitude of the insertion ratio. From Eq. 12, it is therefore possible to write:

$$\alpha_N = \alpha + \alpha_r + \alpha_i \tag{13}$$

where

$$\alpha_N = \ln \left| \frac{E_2'}{E_2} \right| = \text{insertion loss} \tag{14}$$

$$\alpha = \text{attenuation loss} \tag{14a}$$

$$\alpha_r = \ln \left| (1 - \rho^2)^{-1} \right| = \text{reflection loss} \tag{14b}$$

$$\alpha_i = \ln \left| 1 - \rho^2 e^{-2\theta} \right| = \text{interaction loss} \tag{14c}$$

The reflection loss (α_r) represents the mismatch effect at the filter terminals. It yields a correction to the filter attenuation loss which is independent of that loss, since ρ is a function only of Z_o and R_t. The reflection loss is of greatest importance in the filter passband, where the attenuation is zero and the filter loss is primarily the result of mismatch. The filter network is assumed to be nondissipative.

In the filter passband, the reflection loss (Eq. 14b) can be written in terms of z_o by using Eq. 11:

$$\alpha_r = 20 \log \left[\frac{1}{2} \left((z_o)^{1/2} + \frac{1}{(z_o)^{1/2}} \right) \right]^2 \text{ db} \tag{15}$$

Since z_o is always real in the passband, the reflection loss is always positive or zero.

In the stopband, Z_o is imaginary; hence $Z_o = j|Z_o|$. With

$$|z_o| = \frac{|Z_o|}{R_t} \tag{16}$$

Eq. 14b becomes

$$\left.\begin{aligned} \alpha_r &= \ln \left| \frac{1}{4} \left(2 + j|z_o| - \frac{j}{|z_o|} \right) \right| = \ln \frac{1}{4} \left(2 + j|z_o|^2 + \frac{1}{|z_o|^2} \right)^{1/2} \\ &= -\ln(4) + \ln \left(|z_o| + \frac{1}{|z_o|} \right) \end{aligned}\right\} \tag{17}$$

In terms of decibels, Eq. 17 becomes:

$$\alpha_r = -12 + 20 \log \left(|z_o| + \frac{1}{|z_o|} \right) \text{ db} \tag{17a}$$

The minimum value of α_r in the stopband, which occurs when $|z_o| = 1$ or $|Z_o| = R_t$, is seen from Eq. 17a to be

$$\alpha_r \text{ min} = -6 \text{ db}$$

which corresponds to a reflection gain of 6 db. This result can be shown to hold as well

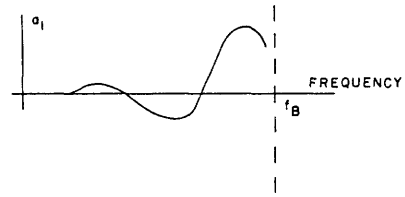

Fig. 6. Variations of interaction loss.

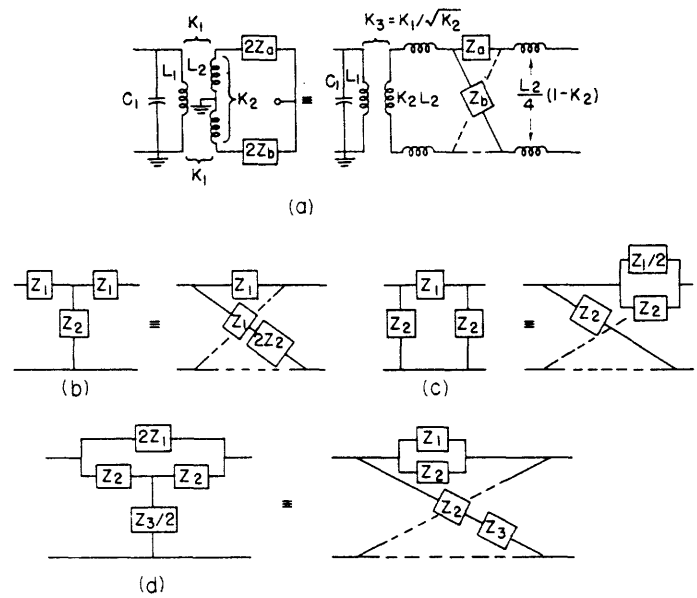

Fig. 7. Lattice equivalents of unbalanced networks: (a) three-winding transformer network; (b) T network; (c) π network; (d) bridged-T network.

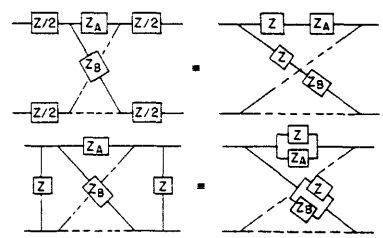

Fig. 8. Lattice network equivalences.

for the dissipative network (22).

The interaction loss (α_i) is a second-order effect, which is generally negligible, but which may be of interest in the vicinity of a cutoff frequency in the filter passband. In the passband, $\theta = j\beta(\alpha = 0)$; and since $e^{-2\beta} = \cos 2\beta - j\sin 2\beta$, Eq. 14c becomes

$$\alpha_i = 20 \log(1 - 2\rho^2 \cos 2\beta + \rho^4)^{1/2} \text{ db} \tag{18}$$

The interaction loss varies in the manner shown in Fig. 6 in the vicinity of a cutoff frequency (f_B). From Eq. 18, the value of α_i is maximum when $\beta = (2n + 1)(\pi/2)$, and minimum when $\beta = n\pi$; $(n = 0, 1, 2, \ldots)$. The interaction loss therefore always lies within the limits

$$20 \log(1 - \rho^2) \leqslant \alpha_i \leqslant 20 \log(1 + \rho^2) \text{ db} \tag{19}$$

2.3 UNBALANCED FORMS

It is sometimes desirable to realize crystal filters in unbalanced form, especially at high frequencies when crystals become very small and division of plating is difficult. The most useful method of obtaining an unbalanced filter, from the point of view of maintaining the generality of the lattice structure, is to employ a three-winding transformer or hybrid coil (5). As shown in Fig. 7a, if the coupling between the secondaries of the transformer is high ($K_2 = 1$), the network becomes equivalent to the symmetrical lattice.

When it is not economical to use the hybrid coil, the filter may be realizable in the form of a T, π, or bridged-T network. The symmetrical lattice equivalents of these networks are shown in Fig. 7b, c, d, and are easily derived by using the lattice equivalence theorems (4) illustrated in Fig. 8. In practice, it is usually found that the characteristics obtainable with T or π networks are too limited to be useful (4). The bridged-T network, on the other hand, is more general than the T or π, and sometimes yields useful results, especially for lowpass, highpass, and band-elimination filters (23).

III. SYNTHESIS OF BANDPASS CRYSTAL FILTERS

3.1 GENERAL PROPERTIES OF BANDPASS FILTERS

Figure 9 illustrates the manner in which crystals, inductances, and capacitors can be combined in symmetrical-lattice configurations to yield bandpass filter characteristics. Curves of series- and shunt-arm reactances, filter attenuation, and image impedance are sketched as functions of frequency for each filter. Filters 1 and 2 are narrow-band filters, limited by crystal zero-pole spacing to bandwidths of less than 0.8 per cent of center frequency for quartz. In each of the remaining filters, inductances (L_o, L'_o) have been added in series or in parallel with the crystal elements to widen the filter passband (4). If quartz is used, bandwidths as large as 13.5 per cent of center frequency are theoretically possible with these combinations.

In order to obtain the highest possible attenuation from each lattice configuration, the passband extends from the lowest critical frequency of the series-arm reactance Z_a (solid line) to the highest critical frequency of the shunt-arm reactance Z_b (dotted line). These two frequencies, f_A and f_B, are called the "cutoff" frequencies. The remaining critical frequencies of Z_a coincide with those of Z_b to produce a continuous passband. Within the passband, the filter attenuation is zero, and the image impedance is resistive (solid line). In the attenuation band, the image impedance is reactive (dotted line), and the attenuation characteristics have a number of infinite peaks which can be no greater than one plus the number of "coincident" frequencies in the passband.

The simplest bandpass crystal filter (filter 1 in Fig. 9) will be referred to as the "basic" section. The attenuation characteristic of the basic section has at most one infinite peak, the position of which may be placed anywhere outside the filter passband by varying the capacitor C'_o. It can be shown (18) that the attenuation characteristic of a filter having n infinite peaks and a bandwidth B is equal to the sum of the

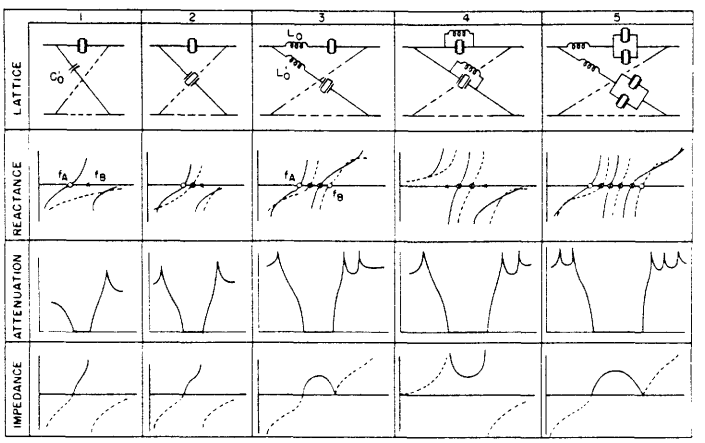

Fig. 9. Bandpass crystal lattice filters.

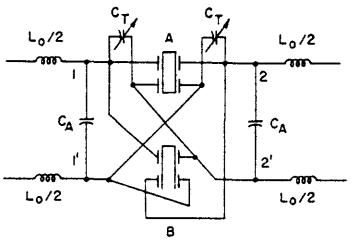

Fig. 10. Wideband lattice filter with divided-plate crystals.

characteristics of n basic sections, wherein each section has a bandwidth B and an attenuation peak corresponding to one of the n peaks of the composite filter.

In practice, filters 3, 4, and 5 are usually realized with the series or parallel inductances equal ($L_o = L'_o$). The inductances can then be placed outside the lattice by following the theorems illustrated in Fig. 8. Some loss in generality of the filter characteristic results if this is done. In the series-inductance case, one attenuation peak must lie at infinite frequency, while in the parallel-inductance case, one peak must lie at zero frequency (23). On the other hand, making the inductances equal saves two inductances, permits the use of divided-plate crystals, and results in a resistance-compensated network, in which the dissipation of the inductances cannot affect the filter selectivity.

Figure 10 illustrates the divided-plate crystal connections for filter 3, when $L_o = L'_o$. The network equivalent of the lattice section between 1-1' and 2-2' is shown in Fig. 3a. The two inductances at either end of the filter are generally wound on one core, reducing the total number of components to two inductances, two divided-plate crystals, and several fixed and variable capacitors.

3.2 OUTLINE OF SYNTHESIS PROCEDURE

The first step in designing a filter that will meet specified attenuation requirements is to determine the number of basic sections which must be combined in order to meet the specifications. An approximation of the basic section characteristic that permits normalization with respect to bandwidth and center frequency will be described. From the graphical addition of these normalized sections, the number and location of infinite attenuation peaks is determined. This information permits the location of the coincident frequencies in the passband. The coincident frequencies and the cutoff frequencies specify completely the pole-zero configuration of the series- and shunt-arm reactances of the lattice. Finally, the values of the elements making up the lattice reactances are determined, within a multiplying constant, from the critical frequencies. We shall describe both an approximate and an exact method of accomplishing each of the outlined steps in the synthesis. The approximate analysis will permit a rapid and a simple solution of the filter synthesis problem with accuracy sufficient to determine whether or not the filter is physically realizable.

3.3 NORMALIZED BASIC SECTION

As shown in Fig. 9, the series arm of the basic section (filter 1) consists of a crystal which has a zero of impedance at f_A and a pole at f_B. Writing the reactance of the

crystal equivalent circuit (Fig. 1b) in terms of f_A and f_B yields

$$Z_a = \frac{-j}{2\pi f\, C_o} \frac{\left(f^2 - f_A^2\right)}{\left(f^2 - f_B^2\right)}$$

The shunt reactance of the basic section is

$$Z_b = \frac{-j}{2\pi f\, C_o'}$$

so that

$$\left(\frac{Z_a}{Z_b}\right)^{1/2} = \left(\frac{C_o'}{C_o}\right)^{1/2} \left(\frac{f^2 - f_A^2}{f^2 - f_B^2}\right)^{1/2} = m^* \left(\frac{f^2 - f_A^2}{f^2 - f_B^2}\right)^{1/2} \tag{20}$$

where m^* is not a function of frequency.

By making use of Eq. 6 and Eq. 7 and recognizing that $\tanh(\theta/2) = 1$ when $f = f_\infty$ (see Fig. 11), it follows that

$$p = \tanh \frac{\theta}{2} = m^* \left(\frac{f^2 - f_A^2}{f^2 - f_B^2}\right)^{1/2} \tag{21}$$

where

$$m^* = \left(\frac{f_\infty^2 - f_B^2}{f_\infty^2 - f_A^2}\right)^{1/2} \tag{22}$$

Equation 21 permits the calculation of all possible attenuation characteristics obtainable with the basic section. Since p is a function of bandwidth and m^* at any frequency, a double infinity of curves would be necessary to cover all possible choices of f_A, f_B, and f_∞. It is possible, however, to find an approximation for p that is independent of bandwidth and center frequency and yet will introduce negligible error in practice. This is done as follows: Define

$$B \equiv f_B - f_A \tag{23}$$

$$f_o \equiv \frac{f_A + f_B}{2} \tag{23a}$$

Now write

$$\left.\begin{aligned} f^2 &= f_o^2 + 2(f - f_o) f_o + (f - f_o)^2 \\ f_\infty^2 &= f_o^2 + 2(f_\infty - f_o) f_o + (f_\infty - f_o)^2 \\ f_A^2 &= f_o^2 - 2\left(\frac{B}{2}\right) f_o + \left(\frac{B}{2}\right)^2 \\ f_B^2 &= f_o^2 + 2\left(\frac{B}{2}\right) f_o + \left(\frac{B}{2}\right)^2 \end{aligned}\right\} \tag{24}$$

and

$$\left.\begin{aligned} f^2 - f_A^2 &= 2f_o \left\{(f - f_o) + \frac{B}{2} + \frac{1}{2f_o}\left[(f - f_o)^2 - \left(\frac{B}{2}\right)^2\right]\right\} \\ &= Bf_o\left[x + 1 + \frac{B_r}{4}(x^2 - 1)\right] \\ &= Bf_o(x+1)\left[1 + \frac{B_r}{4}(x-1)\right] \end{aligned}\right\} \tag{25}$$

where

$$x \equiv \frac{f - f_o}{B/2} \tag{26}$$

$$B_r \equiv \frac{B}{f_o} \quad \text{(relative bandwidth)} \tag{26a}$$

Following a similar process for $f^2 - f_B^2$, $f_\infty^2 - f_A^2$, and $f_\infty^2 - f_B^2$, and substituting the results in Eq. 21 and Eq. 22, yields

$$p^2 = \left[\frac{x_\infty - 1}{x_\infty + 1}\right]\left[\frac{x+1}{x-1}\right]\left[\frac{1 + \frac{B_r}{4}(x_\infty + 1)}{1 + \frac{B_r}{4}(x_\infty - 1)}\right]\left[\frac{1 + \frac{B_r}{4}(x-1)}{1 + \frac{B_r}{4}(x+1)}\right] \tag{27}$$

where

$$x_\infty \equiv \frac{f_\infty - f_o}{B/2}$$

The desired result is now obtained by writing

$$p = p_o(1+\delta) \tag{28}$$

where

$$p_o = m\left(\frac{x+1}{x-1}\right)^{1/2} \tag{29}$$

$$m = \left(\frac{x_\infty - 1}{x_\infty + 1}\right)^{1/2} \tag{29a}$$

and

$$(1+\delta)^2 = \frac{1 + \frac{B_r}{4}(x_\infty + 1)}{1 + \frac{B_r}{4}(x_\infty - 1)} \cdot \frac{1 + \frac{B_r}{4}(x-1)}{1 + \frac{B_r}{4}(x+1)} \tag{30}$$

Equations 29 and 29a permit the attenuation characteristics of the basic section (Fig. 11) to be normalized with respect to bandwidth and center frequency. Furthermore, if

$$F(x) \equiv \left(\frac{x+1}{x-1}\right)^{1/2} \tag{31}$$

then $F(-x) = 1/F(x)$. In addition, $m(-x_\infty) = 1/m(x_\infty)$.

Therefore, if an attenuation curve with $x_\infty = x_{\infty 1}$ is computed, the curve for $x_\infty = -x_{\infty 1}$ is obtained by replacing x by -x (or rotating the characteristic for $x_{\infty 1}$ by 180° about x = 0). Thus, it is sufficient to consider $x_\infty > 1$; that is, attenuation peaks occur above the upper cutoff frequency. All possible characteristics, a number of which are shown in Fig. 12, are then determined.

It is desirable to show that p_o is a sufficiently good approximation for p in all practical cases. Consider the last term on the right of Eq. 30. If $B_r(x+1)/4 \ll 1$, then

$$\frac{1 + \frac{B_r}{4}(x-1)}{1 + \frac{B_r}{4}(x+1)} \approx 1 - \frac{B_r}{2} \tag{32}$$

For narrow-band quartz-crystal filters, $B_r \leqslant 0.8$ per cent = 0.008; Eq. 32 will therefore be an excellent approximation when $x \leqslant 50$. For wideband filters, $B_r \leqslant 0.135$, and Eq. 32 requires $x \leqslant 4$. In either case, the significant portion of the filter attenuation characteristic will lie within the range of x for which Eq. 32 holds.

The first term of Eq. 30 requires somewhat more attention, since x_∞ may fall into three different categories:

A. $B_r(x_\infty - 1)/4 \ll 1$; that is, the attenuation peak falls within the ranges of x mentioned above. This represents the most common case and under these conditions it is easy to show that

$$\delta \approx -\frac{B_r^2}{8} \tag{33}$$

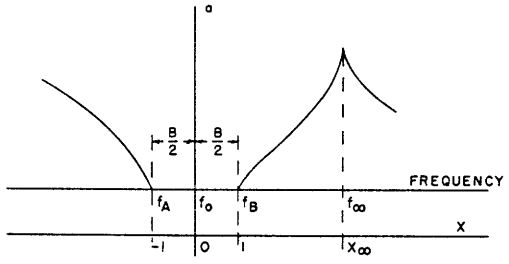

Fig. 11. Basic section characteristic.

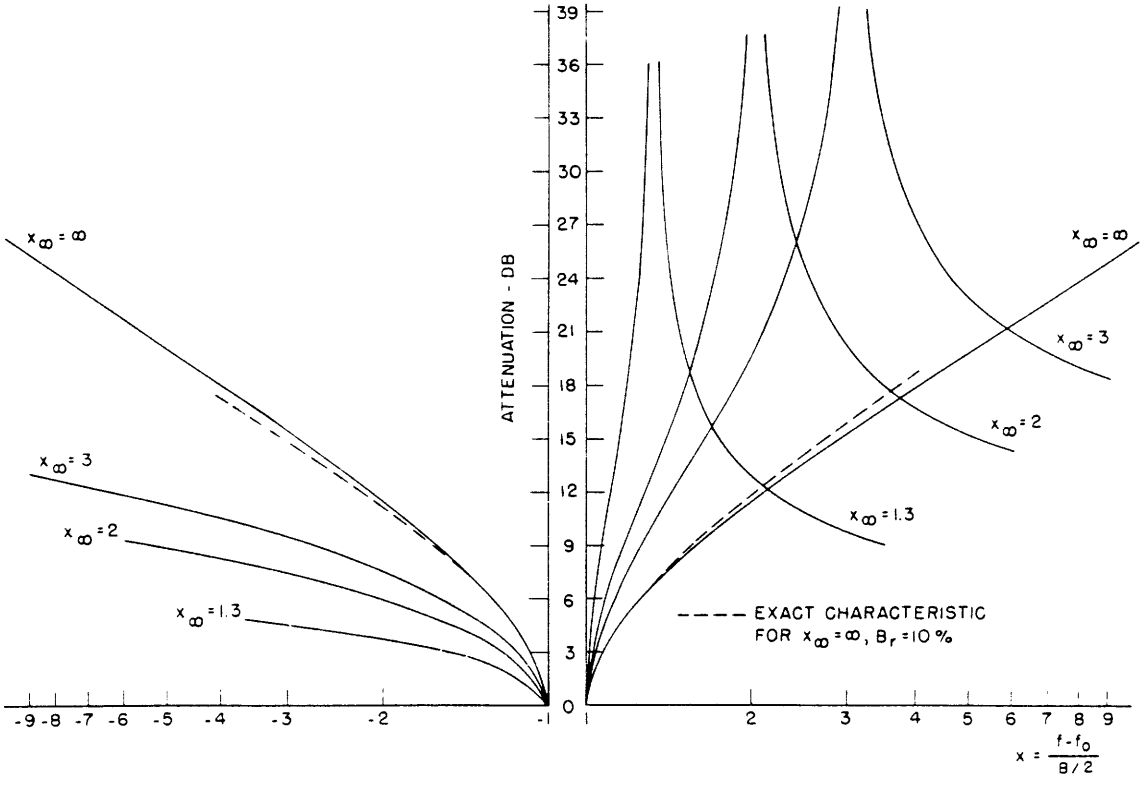

Fig. 12. Normalized basic section attenuation characteristics.

B. $x_\infty = \infty$; (m=1). This condition is equivalent to $f_\infty = \infty$, and results when the series inductances of filters 3 or 5 of Fig. 9 are made equal. In this case, the first term of Eq. 30 is equal to unity and it follows that

$$\delta \approx - \frac{B_r}{4} \tag{34}$$

C. Finally, if $f_\infty = 0$; ($x_\infty = -2/B_r$), as in the case of equal parallel inductances in filter 4 (Fig. 9), then $m \approx 1 + B_r/2$, and if the normalized characteristic corresponding to $x_\infty = \infty$ is used,

$$\delta \approx \frac{3B_r}{4} \tag{35}$$

The approximation for p may be written as an approximation for the attenuation α. From Eq. 9,

$$\alpha = \ln \left| \frac{1 + p}{1 - p} \right| = \ln \left| \frac{1 + p_o(1+\delta)}{1 - p_o(1+\delta)} \right| \tag{36}$$

Since $\delta << 1$,

$$\alpha \approx \alpha_o + \ln \left(1 + \frac{2\delta p_o}{1 - p_o^2} \right) \tag{37}$$

where

$$\alpha_o \equiv \ln \left| \frac{1 + p_o}{1 - p_o} \right| \tag{38}$$

Moreover, since $2\delta p_o / 1 - p_o^2 << 1$,

$$\ln \left(1 + \frac{2\delta p_o}{1 - p_o^2} \right) \approx \frac{2\delta p_o}{1 - p_o^2} \tag{39}$$

If all terms are expressed in decibels, then Eq. 37 becomes

$$\alpha \approx \alpha_o - \frac{17.4\delta}{\left[p_o - (1/p_o) \right]} \text{ db} \tag{40}$$

The order of magnitude of the approximation involved in Eq. 29 can now be seen in terms of α. For example, in case A above, when B_r = 10 per cent, and α_o = 30 db, then α = 30 + 0.16 db, and the error is about 0.5 per cent. Since, in practice, this is an extreme case, it is apparent that in case A a correction need never be made. In case B, for the same relative bandwidth and at x = 4, the correction is approximately 1 db. This correction can be tabulated, since it depends only on the relative bandwidth at any value of x. The exact characteristic is drawn in Fig. 12 as a dotted line for

B_r = 10 per cent. In practice, the $x_\infty = \infty$ characteristic accounts for a relatively small percentage of the total attenuation, so that even in case B the correction can usually be neglected. The same reasoning applies to case C; thus, all practical cases have been considered.

3.4 GRAPHICAL ADDITION OF SECTIONS

Whenever several basic sections are combined to form a filter, the composite attenuation characteristic will have a number of minima, the magnitudes of which must meet specifications given for the filter. By following a procedure developed by Cauer (18, 24) it is possible to determine analytically the configuration of passband critical frequencies (or equivalently, the configuration of attenuation peaks) for which all attenuation minima will have equal values. If this procedure is employed, some readjustments by a cut-and-try process may be necessary to compensate for reflection loss or to satisfy requirements not calling for equiminima behavior.

With the aid of the normalized representation of the basic section previously described, it is often simpler to determine the composite filter characteristic entirely by a trial-and-error process, especially since a given crystal filter is capable of supplying a fixed number of attenuation peaks, some of which may be at zero or at infinite frequency. This process consists of selecting an attenuation-peak configuration, locating the positions of the corresponding attenuation minima by a graphical method derived below, and determining the magnitudes of these minima from a set of normalized characteristics such as that in Fig. 12. The process is repeated until the attenuation at the minima and at other significant points of the filter characteristic is sufficient to satisfy specifications.

It will be shown, in Section IV, that the reflection loss, and to some extent, the interaction loss, of a crystal filter can be determined before the attenuation characteristic is specified. The attenuation minima may therefore be adjusted to satisfy filter specifications that are first corrected for reflection effects.

The procedure for determining graphically the position of attenuation minima is derived as follows: From Eq. 29, Eq. 31, and Eq. 38, the attenuation of a single basic section, neglecting the difference between a and a_o, becomes

$$a = \ln \left| \frac{1 + p_o}{1 - p_o} \right| = \ln \left| \frac{1 + mF}{1 - mF} \right| \tag{41}$$

If n sections are combined, the total attenuation (a_T) becomes:

$$\left.\begin{aligned} a_T &= a_1 + a_2 + a_3 + \ldots + a_n \\ &= \ln|H_1| + \ln|H_2| + \ldots + \ln|H_n| \end{aligned}\right\} \tag{42}$$

where

$$H_n \equiv \frac{1 + m_n F}{1 - m_n F}$$

and

$$m_n = \left(\frac{x_{\infty n} - 1}{x_{\infty n} + 1} \right)^{1/2}$$

The position of the attenuation minima may be determined from the equation

$$\left.\begin{aligned} \frac{d\alpha_T}{dF} &= 0 \\ &= \frac{d}{dF} \ln|H_1| + \frac{d}{dF} \ln|H_2| + \ldots + \frac{d}{dF} \ln|H_n| \end{aligned}\right\} \tag{43}$$

If the required derivatives are taken and reduced to simplest terms, Eq. 43 becomes

$$\frac{d\alpha_T}{dF} = \frac{2m_1}{1 + m_1^2 F^2} + \frac{2m_2}{1 + m_2^2 F^2} + \ldots + \frac{2m_n}{1 + m_n^2 F^2} \tag{44}$$

Equation 44 can be written in terms of x and x_∞ by using Eq. 29a and Eq. 31. The result is the condition that must be satisfied by the abscissa x_m of an attenuation minimum:

$$\frac{\left(x_{\infty 1}^2 - 1\right)^{1/2}}{x_m - x_{\infty 1}} + \frac{\left(x_{\infty 2}^2 - 1\right)^{1/2}}{x_m - x_{\infty 2}} + \ldots + \frac{\left(x_{\infty n}^2 - 1\right)^{1/2}}{x_m - x_{\infty n}} = 0 \tag{45}$$

To solve this equation graphically, it is necessary to plot a series of curves of the function

$$G_n(x) = \frac{\left(x_{\infty n}^2 - 1\right)^{1/2}}{x - x_{\infty n}} \qquad x_{\infty n} > 1 \tag{46}$$

for various values of $x_{\infty n}$. It is interesting to note that

$$G_n(1) = -\frac{1}{m_n}$$

$$G_\infty(x) = -1$$

For negative values of x_∞, the negative square root must be used in Eq. 46 because of the absolute values taken in Eq. 42. That is, if the value of $G_n(x)$ for negative x_∞ is denoted by $G_n^{(-)}(x)$, then

$$G_n^{(-)}(x) = -\frac{\left(x_{\infty n}^2 - 1\right)^{1/2}}{x - x_{\infty n}} \qquad x_{\infty n} \leq 1 \tag{47}$$

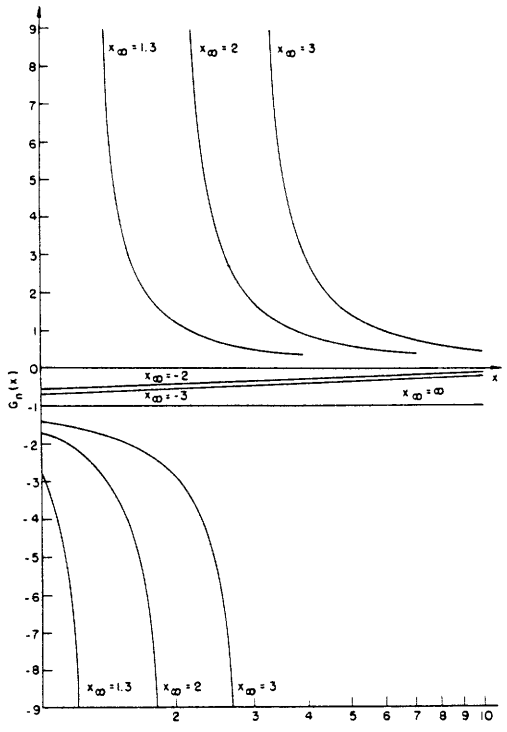

Fig. 13. Curves of $G_n(x)$ versus x.

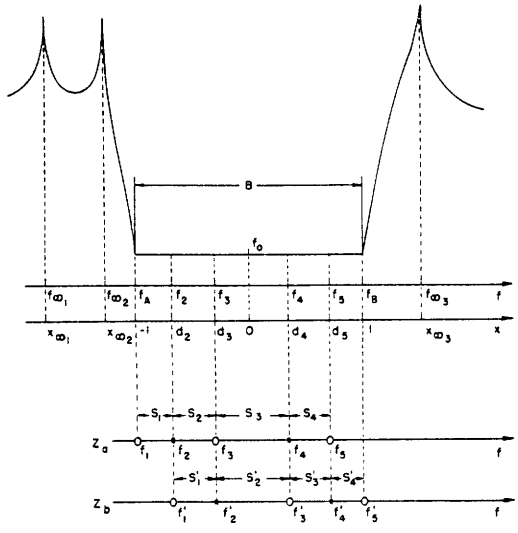

Fig. 14. Notation employed in sections 3.5 – 3.7.

and it follows that

$$G_n^{(-)}(1) = -m\left(\left|x_{\infty n}\right|\right) \tag{48}$$

Curves of $G_n(x)$ versus x for various values of x_∞ are shown in Fig. 13.

3.5 LOCATION OF "COINCIDENT" FREQUENCIES

An exact and an approximate method will be presented for determining the "coincident" frequencies within a filter passband from the frequencies of the infinite peaks in the attenuation band. The notation to be used is given in Fig. 14. The exact method will be presented without proof, since a complete derivation may be found in references 17 and 25.

The most complicated filter to be considered will be a five-peak filter such as filter 5 in Fig. 9. If five basic sections are cascaded, each one described by an equation of the form

$$p_n = m_n^* \left(\frac{f^2 - f_A^2}{f^2 - f_B^2}\right)^{1/2} = \tanh \frac{\theta_n}{2} \tag{49}$$

where

$$m_n^* = \left(\frac{f_{\infty n}^2 - f_B^2}{f_{\infty n}^2 - f_A^2} \right)^{1/2} \tag{49a}$$

it can be shown that the composite filter may be described by

$$p_T = \tanh \frac{(\theta_1 + \theta_2 + \ldots + \theta_5)}{2} = \frac{A_1^* + A_3^* + A_5^*}{1 + A_2^* + A_4^*} \left(\frac{\left(f^2 - f_A^2\right)\left(f^2 - f_3^2\right)^2 \left(f^2 - f_5^2\right)^2}{\left(f^2 - f_B^2\right)\left(f^2 - f_2^2\right)^2 \left(f^2 - f_4^2\right)^2} \right)^{1/2} \tag{50}$$

where $\theta_1 + \theta_2 + \ldots + \theta_5 = \theta_T$ is the composite image propagation constant, and

$$A_1^* = \sum_{n=1}^{5} m_n^* = m_1^* + m_2^* + m_3^* + m_4^* + m_5^*$$

$$A_2^* = \sum_{n=1}^{5} \sum_{o=1}^{5} m_n^* m_o^*; \qquad n \neq o$$

$$A_3^* = \sum_{n} \sum_{o} \sum_{p} m_n^* m_o^* m_p^*; \qquad n \neq o; \quad n \neq p; \quad o \neq p \tag{50a}$$

$$A_4^* = \sum_{n} \sum_{o} \sum_{p} \sum_{q} m_n^* m_o^* m_p^* m_q^*; \qquad n \neq o, p, q; \quad o \neq p, q; \quad p \neq q$$

$$A_5^* = m_1^* m_2^* m_3^* m_4^* m_5^*$$

$$f_2^2 = f_B^2 \left[\frac{1 + \frac{f_A^2}{f_B^2}\left(A_2^* + A_4^* \frac{f_A^2}{f_B^2}\right)}{1 + \frac{A_2^* + \left(A_2^{*2} - 4A_4^*\right)^{1/2}}{2} + \frac{f_A^2}{f_B^2}\left[A_4^* + \frac{A_2^* - \left(A_2^{*2} - 4A_4^*\right)^{1/2}}{2} \right]} \right]$$

$$f_4^2 = f_B^2 \left[\frac{1 + \frac{f_A^2}{f_B^2}\left(A_2^* + A_4^* \frac{f_A^2}{f_B^2}\right)}{1 + \frac{A_2^* - \left(A_2^{*2} - 4A_4^*\right)^{1/2}}{2} + \frac{f_A^2}{f_B^2}\left[A_4^* + \frac{A_2^* + \left(A_2^{*2} - 4A_4^*\right)^{1/2}}{2} \right]} \right] \tag{50b}$$

$$f_3^2 = f_B^2 \left[\frac{A_1^* + \frac{f_A^2}{f_B^2}\left(A_3^* + A_5^* \frac{f_A^2}{f_B^2}\right)}{A_1^* + \frac{A_3^* + \left(A_3^{*2} - 4A_1^* A_5^*\right)^{1/2}}{2} + \frac{f_A^2}{f_B^2}\left[A_5^* + \frac{A_3^* - \left(A_3^{*2} - 4A_1^* A_5^*\right)^{1/2}}{2} \right]} \right]$$

$$f_5^2 = f_B^2 \left[\frac{A_1^* + \frac{f_A^2}{f_B^2}\left(A_3^* + A_5^* \frac{f_A^2}{f_B^2}\right)}{A_1^* + \frac{A_3^* - \left(A_3^{*2} - 4A_1^* A_5^*\right)^{1/2}}{2} + \frac{f_A^2}{f_B^2}\left[A_5^* + \frac{A_3^* + \left(A_3^{*2} - 4A_1^* A_5^*\right)^{1/2}}{2} \right]} \right]$$

If a filter with fewer sections is desired, the results may be obtained by letting some of the m_n^* go to zero. For example, for a three-section filter, $m_4^* = m_5^* = 0$, and Eqs. 50, 50a, and 50b become:

$$p_T = \frac{A_1^* + A_3^*}{1 + A_2^*} \left(\frac{\left(f^2 - f_A^2\right)\left(f^2 - f_3^2\right)^2}{\left(f^2 - f_B^2\right)\left(f^2 - f_2^2\right)^2} \right)^{1/2} \tag{51}$$

where

$$\left.\begin{aligned} A_1^* &= m_1^* + m_2^* + m_3^* \\ A_2^* &= m_1^*\left(m_2^* + m_3^*\right) + m_2^* m_3^* \\ A_3^* &= m_1^* m_2^* m_3^* \\ A_4^* &= A_5^* = 0 \end{aligned}\right\} \tag{51a}$$

$$\left.\begin{aligned} f_2^2 &= \frac{f_B^2 + A_2^* f_A^2}{1 + A_2^*} \\ f_3^2 &= \frac{A_1^* f_B^2 + A_3^* f_A^2}{A_1^* + A_3^*} \\ f_4^2 &= f_5^2 = f_B^2 \end{aligned}\right\} \tag{51b}$$

The approximate solution corresponding to Eqs. 50, 50a, and 50b is derived in Appendix A of reference 38. The results will be given here.

If five basic sections are cascaded, each one described by a normalized equation of the form

$$p_{on} = m_n\left(\frac{x + 1}{x - 1}\right)^{1/2} \tag{52}$$

where

$$m_n = \left(\frac{x_{\infty n} - 1}{x_{\infty n} + 1}\right)^{1/2} \qquad n = 1, 2, \ldots, 5 \tag{52a}$$

the composite filter may be described by

$$p_{oT} = \frac{A_1 + A_3 + A_5}{1 + A_2 + A_4} \left(\frac{(x+1)\,(x - d_3)^2\,(x - d_5)^2}{(x-1)\,(x - d_2)^2\,(x - d_4)^2} \right)^{1/2} \tag{53}$$

where A_1 through A_5 are defined by Eq. 50a, if the asterisks are omitted, and

$$d_i = \frac{f_i - f_o}{B/2}; \qquad i = 2, 3, 4, 5 \tag{54}$$

In terms of the values of A_1, A_2, ..., A_5, the values of d_i are given by

$$\left.\begin{aligned} d_2 &= \frac{1 + A_4 - A_2}{1 - A_4 + \left(A_2^2 - 4A_4\right)^{1/2}} \\ d_4 &= \frac{1 + A_4 - A_2}{1 - A_4 - \left(A_2^2 - 4A_4\right)^{1/2}} \\ d_3 &= \frac{A_1 + A_5 - A_3}{A_1 - A_5 + \left(A_3^2 - 4A_1 A_5\right)^{1/2}} \\ d_5 &= \frac{A_1 + A_5 - A_3}{A_1 - A_5 - \left(A_3^2 - 4A_1 A_5\right)^{1/2}} \end{aligned}\right\} \tag{55}$$

Finally, for a three-section filter

$$p_{oT} = \frac{A_1 + A_3}{1 + A_2}\left(\frac{(x+1)\,(x - d_3)^2}{(x-1)\,(x - d_2)^2}\right)^{1/2} \tag{56}$$

$$\left.\begin{aligned} A_1 &= m_1 + m_2 + m_3 \\ A_2 &= m_1(m_2 + m_3) + m_2 m_3 \\ A_3 &= m_1 m_2 m_3 \\ A_4 &= A_5 = 0 \end{aligned}\right\} \tag{56a}$$

$$\left.\begin{aligned} d_2 &= \frac{1 - A_2}{1 + A_2} \qquad d_3 = \frac{A_1 - A_3}{A_1 + A_3} \\ d_4 &= d_5 = 1 \end{aligned}\right\} \tag{56b}$$

Note: For $f_\infty = \infty$: $x_\infty = \infty$; $m = 1$
For $f_\infty = 0$: $x_\infty = -2/B_r$; $m \approx 1 + B_r/2$

3.6 ELEMENT VALUES OF FILTER REACTANCES

When the passband "coincident" frequencies are determined, the critical frequency patterns of the filter reactance elements are likewise determined. For example, Fig. 14 shows the zero-pole configurations for Z_a and Z_b in the case of filter 5 in Fig. 9. Note the use of the prime to distinguish quantities related to Z_b.

The synthesis procedure is complete when the element values of Z_a and Z_b are determined from the corresponding critical frequencies. This determination can be accomplished by exact or by approximate methods. The calculations involved are described in Appendix I; only the results are presented in this section.

The reactances to be considered are: (a) crystal, (b) inductance in series with crystal, and (c) inductance in parallel with crystal. A complete list of filter reactances, including combinations containing two crystals in parallel, is given in Article 3.6 of reference 38. The three combinations listed above are those most commonly encountered in crystal-filter synthesis.

All element values will be determined in terms of the crystal shunt capacitance C_o, which is limited by various crystallographic considerations to a relatively small range of values. Within this range of values, C_o may be chosen to fix the filter image impedance.

A crystal unit will be specified by its resonant frequency (f_a), and its ratio of capacitances (C_o/C_1). The ratio of capacitances determines whether or not the crystal can be obtained, since the realizability criterion states that

$$r = C_o/C_1 \geq r_x$$

where r_x depends upon the crystal cut employed. The crystal series capacitance (C_1), or inductance (L_1), is determined (in terms of C_o) if f_a and r are fixed, since

$$C_1 = \frac{C_o}{r} \tag{57}$$

$$L_1 = \frac{1}{4\pi^2 f_a^2 C_1} = \frac{r}{4\pi^2 f_a^2 C_o} \tag{57a}$$

An inductance (L_o) placed in series or in parallel with crystal units will be determined by the frequency at which it resonates C_o. This frequency will be called f_a, so that

$$L_o = \frac{1}{4\pi^2 f_a^2 C_o} \tag{58}$$

All approximate data represent only a first degree of approximation, since these data will be used for rapid calculation. The element values are calculated from the spacing (S_i) between the reactance critical frequencies. The necessary values of S_i

may be calculated from the values of d_i (Fig. 14) as follows:

$$\left.\begin{aligned} S_1 &= \frac{B}{2}(d_2 + 1) \\ S_2 = S'_1 &= \frac{B}{2}(d_3 - d_2) \\ S_3 = S'_2 &= \frac{B}{2}(d_4 - d_3) \\ S_4 = S'_3 &= \frac{B}{2}(d_5 - d_4) \\ S'_4 &= \frac{B}{2}(1 - d_5) \end{aligned}\right\} \tag{59}$$

a. Crystal

$$Z_a = \frac{-j}{2\pi f C_o} \frac{f^2 - f_a^2}{f^2 - f_b^2} \tag{60}$$

$C_o = C_{ox} + C_A$, where C_{ox} is the crystal-unit static capacitance and C_A is any added parallel capacitance as shown in Fig. 15.

$$s_a = f_b - f_a \tag{61}$$

$$r = \frac{f_a^2}{f_b^2 - f_a^2} \approx \frac{f_a}{2S_a} \tag{62}$$

From Eq. 57,

$$C_1 = C_o \frac{f_b^2 - f_a^2}{f_a^2} \approx \frac{2C_o S_a}{f_a} \tag{63}$$

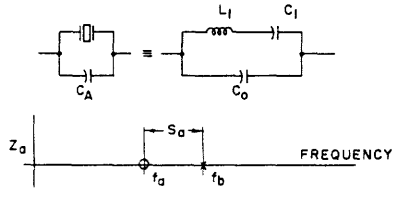

Fig. 15. Reactance of crystal unit.

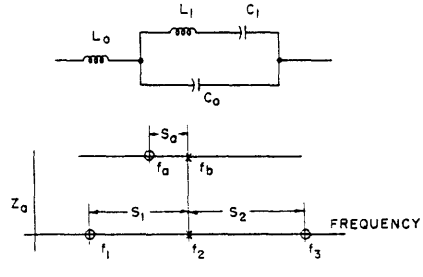

Fig. 16. Inductance in series with crystal.

b. Inductance in series with crystal

$$Z_a = j2\pi fL_o \frac{\left(f^2 - f_1^2\right)\left(f^2 - f_3^2\right)}{f^2\left(f^2 - f_2^2\right)} \tag{64}$$

From Appendix I (Eq. 188):

$$S_a \approx \frac{2S_1S_2}{f_2} \qquad \text{(see Fig. 16)} \tag{65}$$

and

$$f_a = \left(f_1^2 + f_3^2 - f_2^2\right)^{1/2} \approx f_2 + (S_2 - S_1) \tag{66}$$

Repeating Eq. 58:

$$L_o = \frac{1}{4\pi^2 f_a^2 C_o}$$

$$f_a = \frac{f_1 f_3}{f_a} \approx f_2 - \frac{2S_1S_2}{f_2} \tag{67}$$

$$r = \frac{f_a^2}{f_2^2 - f_a^2} \approx \frac{f_2^2}{4S_1S_2} \tag{68}$$

$$C_1 = C_o \frac{\left(f_2^2 - f_a^2\right)}{f_a^2} \approx C_o \frac{4S_1S_2}{f_2^2} \tag{69}$$

c. Inductance in parallel with crystal

$$Z_a = \frac{-j}{2\pi fC_o} \frac{f^2\left(f^2 - f_2^2\right)}{\left(f^2 - f_1^2\right)\left(f^2 - f_3^2\right)} \tag{70}$$

$$f_a = f_2 \qquad \text{(see Fig. 17)} \tag{71}$$

$$f_a = \frac{f_1 f_3}{f_a} \approx f_2 + (S_2 - S_1) \tag{72}$$

Repeating Eq. 58:

$$L_o = \frac{1}{4\pi^2 f_a^2 C_o}$$

$$f_b = \left(f_1^2 + f_3^2 - f_a^2\right)^{1/2} \tag{73}$$

$$r = \frac{f_a^2}{f_b^2 - f_a^2} \approx \frac{f_a^2}{4S_1S_2} \tag{74}$$

$$C_1 = C_o \frac{\left(f_b^2 - f_a^2\right)}{f_a^2} \approx C_o \frac{4S_1S_2}{f_a^2} \tag{75}$$

3.7 SUMMARY

The results of the previous sections will be combined to illustrate the synthesis of the bandpass filters shown in Fig. 9. Specifically, filter 2 (narrow-band), and filter 3 (wideband) will be considered.

The method of determining the element values of Z_a from the corresponding critical frequencies, or zero-pole spacings has just been described. The elements of Z_b may be determined in a similar manner, but it is more instructive to express the parameters of Z_b as a ratio of the corresponding values in Z_a. For example, the ratio C_o/C_o' is the quantity that is adjusted during filter alignment to set the positions of the attenuation peaks (15). The ratio C_1/C_1', moreover, is important for two reasons. First of all, this ratio will in most cases uniquely determine the relative positions of the attenuation peaks in a filter. Since it cannot be varied without changing the crystal units, the ratio C_1/C_1' must be set by the crystal grinder to very close tolerances. This point will be discussed further. The other reason for the importance of this ratio is one of physical realizability. In grinding a pair of crystal units for a filter, the ratio C_1/C_1' is determined approximately by the ratio of the thicknesses of the quartz plates. Because of mechanical considerations, this ratio may lie in the range 0.1 to 10, approximately. When the ratio required by the filter design is outside of this range, as might be the case in a filter with all attenuation peaks on one side of the passband, a capacitor could be placed in series with one of the crystals to lower its capacitance (15, 38). However, the series capacitor will raise r, and therefore decrease the bandwidth obtainable from the filter.

The problem discussed above, which is peculiar to crystal filter synthesis, makes the approximate method of analysis particularly desirable.

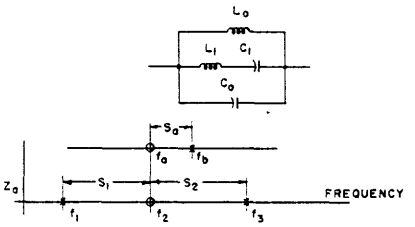

Fig. 17. Inductance in parallel with crystal.

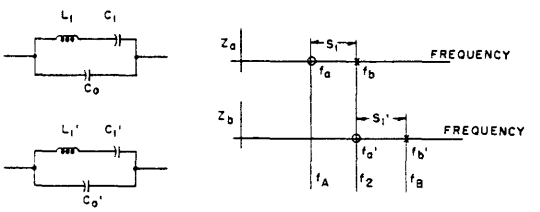

Fig. 18. Narrow-band filter.

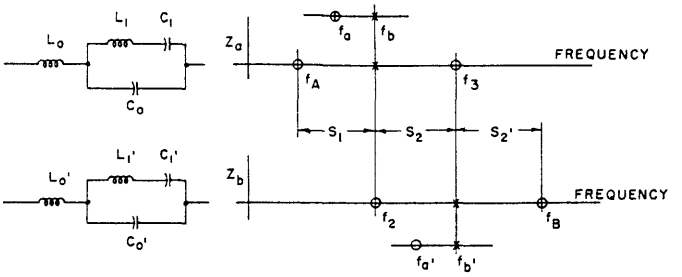

Fig. 19. Wideband filter.

a. Narrow-band two-section filter

This filter will be of the type shown as filter 2 in Fig. 9. The reactances of the lattice arms are shown in Fig. 18 with the corresponding critical frequency configurations. From Eq. 60

$$p = \left(\frac{Z_a}{Z_b}\right)^{1/2} = \left(\frac{C_o'}{C_o}\right)^{1/2} \left(\frac{\left(f^2 - f_A^2\right)\left(f^2 - f_B^2\right)}{\left(f^2 - f_2^2\right)^2}\right)^{1/2} \tag{76}$$

$$Z_o = (Z_a Z_b)^{1/2} = \frac{j}{2\pi f (C_o C_o')^{1/2}} \left(\frac{f^2 - f_A^2}{f^2 - f_B^2}\right)^{1/2} \tag{77}$$

The steps involved in the synthesis procedure are listed in Table I, along with the corresponding formulas. The information available before step 1 is: f_A, f_B, $f_{\infty 1}$, $f_{\infty 2}$, (or $x_{\infty 1}$, $x_{\infty 2}$).

b. Wideband three-section filter

The filter will be of the type shown as filter 3 in Fig. 9. The reactances and corresponding zero-pole configurations of Z_a and Z_b are shown in Fig. 19. From Eq. 64

$$p = \left(\frac{Z_a}{Z_b}\right)^{1/2} = \left(\frac{L_o}{L_o'}\right)^{1/2} \left(\frac{\left(f^2 - f_A^2\right)\left(f^2 - f_3^2\right)^2}{\left(f^2 - f_B^2\right)\left(f^2 - f_2^2\right)^2}\right)^{1/2} \tag{78}$$

$$Z_o = (Z_a Z_b)^{1/2} = j2\pi f (L_o L_o')^{1/2} \left(\frac{\left(f^2 - f_A^2\right)\left(f^2 - f_B^2\right)}{(f^2)^2}\right)^{1/2} \tag{79}$$

The steps necessary to accomplish the synthesis of this filter are listed in Table II. The information available before step 1 is: f_A, f_B, $f_{\infty 1}$, $f_{\infty 2}$, $f_{\infty 3}$ (or $x_{\infty 1}$, $x_{\infty 2}$, $x_{\infty 3}$).

Table I. Synthesis of Narrow-Band Two-Section Lattice Filter.

Step	Quantity	Exact		Approximate	
		Formula	Source	Formula	Source
1	m_1^*, m_1 m_2^*, m_2	$\left(\frac{f^2_{\infty 1,2} - f_B^2}{f^2_{\infty 1,2} - f_A^2}\right)^{1/2}$	(49a)	$\left(\frac{x_{\infty 1,2} - 1}{x_{\infty 1,2} + 1}\right)^{1/2}$	(52a)
2	A_1^*, A_1 A_2^*, A_2	$m_1^* + m_2^*$ $m_1^* m_2^*$	(51a)	$m_1 + m_2$ $m_1 m_2$	(56a)
3	f_2 d_2	$\left[\left(f_B^2 + A_2^* f_A^2\right)/1 + A_2^*\right]^{1/2}$	(51b)	$(1 - A_2)/(1 + A_2)$	(56b)
4	S_1 S_1'			$B/2 \cdot (d_2 + 1)$ $B/2 \cdot (1 - d_2)$	(59)
5	$f_a; f_a'$	$f_A; f_2$	Fig. 18	$f_A; f_A + S_1$	Fig. 18
6	$f_b; f_b'$	$f_2; f_B$	Fig. 18		
7	C_o/C_o'	$\left(\frac{1 + A_2^*}{A_1^*}\right)^2$	(51) (76)	$\left(\frac{1 + A_2}{A_1}\right)^2$	(56) (76)
8	C_1/C_1'	$\frac{C_o}{C_o'}\left[\frac{f_a'^2\left(f_b^2 - f_a^2\right)}{f_a^2\left(f_b'^2 - f_a'^2\right)}\right]$	(63)	$\frac{C_o}{C_o'} \cdot \frac{S_1}{S_1'}$	(63)
9	r r'	$f_a^2/\left(f_b^2 - f_a^2\right)$ $f_a'^2/\left(f_b'^2 - f_a'^2\right)$	(62)	$f_a/2S_1$ $f_a'/2S_1'$	(62)
10	C_1	$C_o \frac{f_b^2 - f_a^2}{f_a^2}$	(63)	$C_o \frac{2S_1}{f_a}$	(63)

Table II. Synthesis of Wideband Three-Section Lattice Filter.

Step	Quantity	Exact		Approximate	
		Formula	Source	Formula	Source
1	m_1^*, m_2^*, m_3^* m_1, m_2, m_3	$\left(\frac{f_{\infty n}^2 - f_B^2}{f_{\infty n}^2 - f_A^2}\right)^{1/2}$	(49a)	$\left(\frac{x_{\infty n} - 1}{x_{\infty n} + 1}\right)^{1/2}$	(52a)
2	A_1, A_2, A_3	Σm_n^*, etc.	(51a)	Σm_n, etc.	(56a)
3	f_2; d_2 f_3; d_3	$\left(\frac{f_B^2 + A_2^* f_A^2}{1 + A_2^*}\right)^{1/2}$ etc.	(51b)	$(1 - A_2)/(1 + A_2)$ $(A_1 - A_3)/(A_1 + A_3)$	(56b)
4	S_1, S_2, S_2'			$B/2 \cdot (d_2 + 1)$, etc.	(59)
5	f_a f_a'	$\left(f_A^2 + f_3^2 - f_2^2\right)^{1/2}$ $\left(f_2^2 + f_B^2 - f_3^2\right)^{1/2}$	(66)	$f_A + S_2$	(66)
6	f_a f_a'	$f_A f_3 / f_a$ $f_2 f_B / f_a'$	(67)	$f_2 - \frac{2S_1S_2}{f_2}$ $f_3 - \frac{2S_2S_2'}{f_3}$	(67) Fig. 19
7	L_o/L_o'	$\left(\frac{A_1^* + A_3^*}{1 + A_2^*}\right)^2$	(51) (78)	$\left(\frac{A_1 + A_3}{1 + A_2}\right)^2$	(56) (78)
8	C_o/C_o'	$\frac{L_o'}{L_o} \cdot \frac{f_a'^2}{f_a^2}$	(58)	$\frac{L_o'}{L_o}$	(58)
9	C_1/C_1'	$\frac{C_o}{C_o'}\left[\frac{f_a'^2\left(f_2^2 - f_a^2\right)}{f_a^2\left(f_3^2 - f_a'^2\right)}\right]$	(63)	$\frac{L_o'}{L_o}\ \frac{S_1}{S_2'}$	(69)
10	r, r'	$f_a^2/\left(f_2^2 - f_a^2\right)$, etc.	(68)	$\frac{f_2^2}{4S_1S_2}, \frac{f_3^2}{4S_2S_2'}$	(68)
11	C_1	$C_o \frac{f_2^2 - f_a^2}{f_a^2}$	(69)	$C_o \frac{4S_1S_2}{f_2^2}$	(69)
12	L_o	$1/4\pi^2 f_a^2 C_o$	(58)	$1/4\pi^2 f_a^2 C_o$	(58)

It is interesting to note that for filters with symmetrical attenuation characteristics (about $f = f_o$, or $x = 0$), it is sometimes possible to express the maximum bandwidth (which depends upon r) in terms of the locations of attenuation peaks. In such cases, a great deal of information can be obtained without necessitating even an approximate synthesis. The use of the normalization technique to accomplish this analysis and its use in determining the characteristics obtainable with crystal filters that are realized in unbalanced form are discussed in Chapter V of reference 38.

IV. INSERTION LOSS OF BANDPASS FILTERS

4.1 IMAGE IMPEDANCE

One of the general properties of the crystal lattice filters described in Section III, is the arrangement of the critical frequencies of Z_a and Z_b. With the exception of the cutoff frequencies f_A and f_B, every zero of Z_a is coincident with a pole of Z_b, or vice versa. Furthermore, since the coincident frequencies are located within the passband, it follows that the image impedance

$$Z_o = (Z_a Z_b)^{1/2} \tag{80}$$

can have a frequency dependence that involves only f_A and f_B. Therefore Z_o can be classified according to three types, depending on the nature of f_A and f_B:

Type I: f_A = zero; f_B = pole

$$Z_{o1} = \frac{M_1}{f}\left(\frac{f^2 - f_A^2}{f_B^2 - f^2}\right)^{1/2} \tag{81}$$

Type II: $f_A = f_B$ = zero

$$Z_{o2} = \frac{M_2}{f}\left(\left(f^2 - f_A^2\right)\left(f_B^2 - f^2\right)\right)^{1/2} \tag{82}$$

Type III: $f_A = f_B$ = pole

$$Z_{o3} = M_3 f \frac{1}{\left(\left(f^2 - f_A^2\right)\left(f_B^2 - f^2\right)\right)^{1/2}} \tag{83}$$

where M_1, M_2, and M_3 are constants that depend on the filter configuration.

Type I would yield an image impedance that is the reciprocal of Z_{o1}, and is not significant.

If we use the normalization procedure described in connection with the basic section, it is possible to write

$$f^2 - f_A^2 = B\, f_o (1+x)\left[1 + \frac{B_r}{4}(x-1)\right] \tag{84}$$

$$f_B^2 - f^2 = B\, f_o (1-x)\left[1 + \frac{B_r}{4}(x+1)\right] \tag{84a}$$

where use has been made of Eq. 23 to Eq. 26a. Substituting Eq. 84 and Eq. 84a in Eq. 81, Eq. 82, and Eq. 83, we obtain

$$Z_{o1} \approx \frac{M_1}{f_o}\left(\frac{1+x}{1-x}\right)^{1/2}\left[1 - \frac{B_r}{4}(2x+1)\right] \tag{85}$$

$$Z_{o2} \approx M_2 f_o B_r (1-x^2)^{1/2}\left(1 - \frac{B_r}{4}x\right) \tag{86}$$

$$Z_{o3} \approx \frac{M_3}{f_o B_r}\frac{1}{(1-x^2)^{1/2}}\left(1 + \frac{B_r}{4}x\right) \tag{87}$$

Since the last term in each equation above is negligible in the neighborhood of the filter passband, the normalized image impedances may be written:

$$Z_{o1} \approx R_{o1}\left(\frac{1+x}{1-x}\right)^{1/2} \tag{88}$$

$$Z_{o2} \approx R_{o2}(1-x^2)^{1/2} \tag{89}$$

$$Z_{o3} \approx \frac{R_{o3}}{(1-x^2)^{1/2}} \tag{90}$$

where R_o is the impedance at $f = f_o (x = 0)$, and

$$R_{o1} = \frac{M_1}{f_o} \tag{91}$$

$$R_{o2} = M_2 f_o B_r \tag{92}$$

$$R_{o3} = \frac{M_3}{f_o B_r} \tag{93}$$

The image impedances of Types I and II are plotted as a function of x in Fig. 20.

Table III. Image Impedance of Bandpass Filters.

Filter No.	Image Impedance	R_o
1, 2	$\frac{1}{2\pi f (C_o C_o')^{1/2}}\left(\frac{f^2 - f_A^2}{f_B^2 - f^2}\right)^{1/2}$	$\frac{1}{2\pi f_o C_o}\left(\frac{C_o}{C_o'}\right)^{1/2}$
3, 5	$\frac{2\pi (L_o L_o')^{1/2}}{f}\left(\left(f^2 - f_A^2\right)\left(f_B^2 - f^2\right)\right)^{1/2}$	$\frac{1}{2\pi f_o C_o}\frac{B_r}{(L_o/L_o')^{1/2}}$
4	$\frac{f}{2\pi (C_o C_o')^{1/2}}\frac{1}{\left(\left(f^2 - f_A^2\right)\left(f_B^2 - f^2\right)\right)^{1/2}}$	$\frac{1}{2\pi f_o C_o}\frac{(C_o/C_o')^{1/2}}{B_r}$

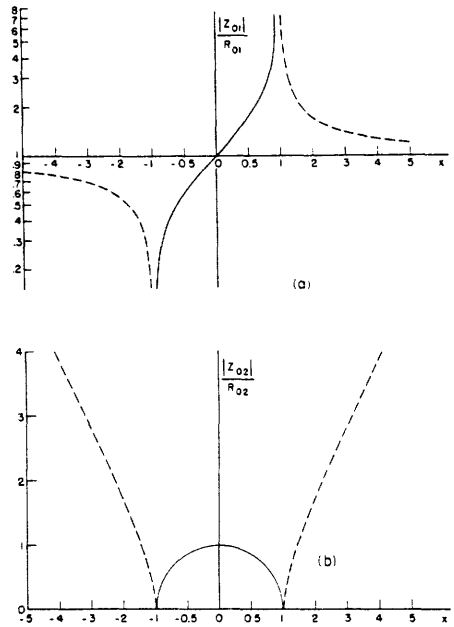

Fig. 20. Image impedance characteristics of bandpass filters.

As in Fig. 9, the solid line represents resistive impedance, and the dotted line reactive impedance. Since $|Z_{03}|/R_{03} = R_{02}/|Z_{02}|$, the impedance characteristic of Type III is the reciprocal of Fig. 20b.

Equations 81-83 and Eqs. 91-93 can be applied to the bandpass filters shown in Fig. 9. The results are shown in Table III.

In each case, the image impedance is obtained by substituting in Eq. 80 the values of Z_a given in section 3.6 and the corresponding values of Z_b. The values of R_o given for filters 3 and 5 would be

$$R_{o2} = 2\pi f_o L_o \frac{B_r}{(L_o/L'_o)^{1/2}} \tag{94}$$

if Eq. 82 and Eq. 92 are used. However, by making use of Eq. 58, and neglecting the difference between f_o and f_a, Eq. 94 may be written in the form shown in Table III.

The formulas for R_o given in Table III may be used to determine the value of C_o necessary to provide a particular image impedance.

Alternatively, the image impedance can be expressed in the terms of crystal inductance. It is only necessary to use Eq. 57a and to note that $f_a \approx f_o$; then it follows that

$$\frac{1}{2\pi f_o C_o} \approx \frac{2\pi f_o L_1}{r} \tag{95}$$

Substituting Eq. 95 in column 3 of Table III yields the desired expression for R_o in terms of L_1 for each impedance type.

4.2 PHASE CHARACTERISTICS

Crystal bandpass filters are rarely, if ever, designed for specified phase characteristics. However, when it is important to determine the exact behavior of the filter in the passband, the interaction loss, which depends upon the phase characteristic, must be calculated.

Within the filter passband $|x| \leq 1$, so that the normalized approximate expressions for the image propagation constant θ may be used with negligible error. Making use of Eq. 45 and Eq. 29a, it follows that

$$\theta = \alpha + j\beta = 2 \tanh^{-1} p_o \tag{96}$$

where

β = image phase constant

and

$$p_o = m\left(\frac{x+1}{x-1}\right)^{1/2} \tag{97}$$

where

$$m = \left(\frac{x_\infty - 1}{x_\infty + 1}\right)^{1/2} \tag{98}$$

In the passband $\alpha = 0$, and

$$\tanh \frac{\theta}{2} = \tanh j\frac{\beta}{2} = j \tan \frac{\beta}{2}$$

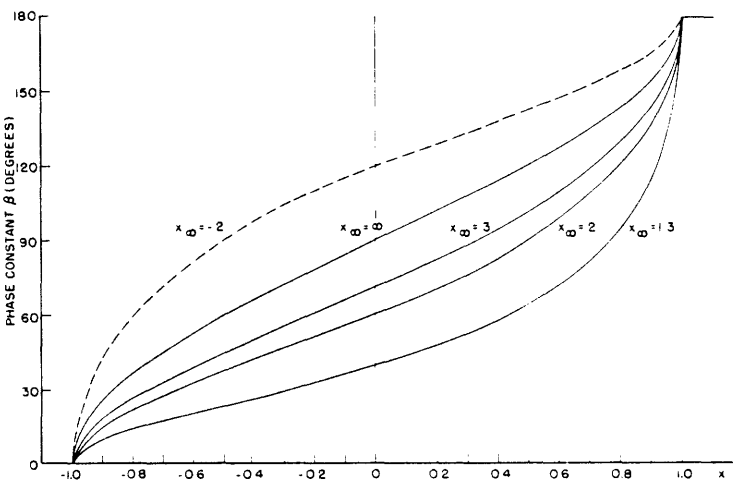

Fig. 21. Phase characteristics of basic section.

so that

$$\beta = 2 \tan^{-1} m\left(\frac{1+x}{1-x}\right)^{1/2} \tag{99}$$

Curves of β versus x are plotted in Fig. 21 for various values of x_∞. The characteristics for x_∞ negative (one of which is shown dotted in Fig. 21) are obtained from the expression

$$\beta_n^{(-1)}(x) = 180° - \beta_n(-x) \tag{100}$$

That is, the phase constant at any value of x for $x_\infty = -x_{\infty n}$, which is denoted by $\beta_n^{(-1)}(x)$, is equal to 180° minus the phase constant at (-x) for $x_\infty = x_{\infty n}$. Equation 100 is easily derived by replacing x and x_∞ by (-x) and $(-x_\infty)$ in Eq. 97 and Eq. 98.

The composite phase constant (β_T) for a number of cascaded basic sections is, of course, the sum of the phase constants for the individual sections at any value of x.

4.3 REFLECTION AND INTERACTION LOSSES

When the results obtained in section 2.2 are repeated, the insertion loss (a_N) introduced by a symmetrical filter terminated in R_t is given by

$$a_N = a + a_r + a_i \tag{101}$$

where

$$a_r = \ln \left| (1 - \rho^2)^{-1} \right| = \text{reflection loss} \tag{102}$$

$$a_i = \ln \left| 1 - \rho^2 e^{-2\theta_T} \right| = \text{interaction loss} \tag{102a}$$

and

$$\rho = \frac{1 - z_o}{1 + z_o} \tag{103}$$

where

$$z_o = \frac{Z_o}{R_t} \tag{104}$$

In the filter passband, Z_o is real, and Eq. 102 may be written

$$a_r = 20 \log \left[\frac{1}{2} \left((z_o)^{1/2} + \frac{1}{(z_o)^{1/2}} \right) \right]^2 \text{ db} \tag{105}$$

In the attenuation band, Z_o is imaginary and Eq. 102 becomes

$$a_r = -12 + 20 \log \left(|z_o| + \frac{1}{|z_o|} \right) \text{ db} \tag{106}$$

where

$$|z_o| = |Z_o|/R_t$$

It should be noted at this point that the reflection loss given by Eq. 102 is a function only of the image impedance and the terminating resistance of a given filter. Moreover, as explained above, the image impedance of a crystal filter is independent of the number of basic sections making up the composite filter. By making use of the normalized representations of $|Z_o|/R_o$ plotted in Fig. 20 it is therefore possible to determine a_r for all possible crystal filters by computing the reflection loss for Z_{o1} (narrow-band filters) and for Z_{o2} (wideband filters). The resultant values of a_r versus x may be subtracted from a given set of filter specifications, after which the filter is designed for an image attenuation that meets the adjusted specifications.

A discussion of the interaction loss was given in section 2.2, wherein it was shown that a_i is significant only in the passband and is given in that region by

$$a_i = 20 \log(1 - 2\rho^2 \cos 2\beta_T + \rho^4)^{1/2} \text{ db} \qquad (107)$$

It is obvious from the symmetry of $|Z_{o1}|/R_{o1}$ about x = 0 and about $|Z_{o1}|/R_{o1} = 1$ in Fig. 20a that the insertion loss will be symmetrical about x = 0 if $R_t = R_{o1}$. If a constant a_o is defined by $a_o = R_t/R_o$, then the best terminal condition for a filter with an image impedance of Type I corresponds to $a_o = 1$. The reflection loss corresponding to this condition is shown in Fig. 22a. We see that a reflection gain of 6 db occurs over most of the filter attenuation band. The dotted line in Fig. 22a shows the attenuation characteristic corrected for interaction loss in a narrow-band filter composed of two basic sections, with attenuation peaks symmetrically located about x = 0 and $|x_\infty| \geq 10$.

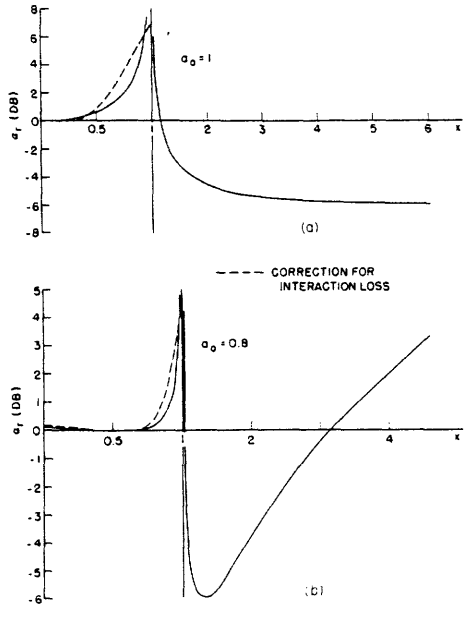

Fig. 22. Reflection loss of bandpass filters.

The image impedance of Type II, shown in Fig. 20b, is identical with the midseries image impedance of a constant-k lowpass filter (26). A filter having this type of impedance is best terminated by a resistance somewhat less than R_o. It can be shown (27) that the most satisfactory terminations correspond to values of a_o in the vicinity of 0.7 and 0.8. The reflection loss for $a_o = 0.8$ is shown in Fig. 22b. The dotted line represents the total insertion loss in the passband for a wideband filter composed of three basic sections with $x_{\infty 1} = -2$, $x_{\infty 2} = +2$, $x_{\infty 3} = \infty$.

Although it is rarely necessary to calculate

the interaction loss over the entire passband, it is frequently desirable to know the filter insertion loss at the cutoff frequencies ($x = \pm 1$). The expressions for reflection and interaction loss given by Eqs. 102 and 102a do not hold at the cutoff frequencies, but the combined loss given by

$$a_N = \ln \left| \frac{1 - \rho^2 e^{-2\theta_T}}{1 - \rho^2} \right| \tag{108}$$

must be finite at $x = \pm 1$.

To calculate this loss, use is made of the normalized expression for the composite image propagation constant θ_T. From Eq. 8 and Eq. 53

$$e^{-2\theta_T} = \left[\frac{1 - p_{oT}}{1 + p_{oT}} \right]^2 \tag{109}$$

where

$$p_{oT} = \frac{A_1 + A_3 + A_5}{1 + A_2 + A_4} \left(\frac{x+1}{x-1} \right)^{1/2} \frac{(x - d_3)(x - d_5)}{(x - d_2)(x - d_4)} \tag{110}$$

From Eq. 110 it follows that in the vicinity of the cutoff frequencies ($x = \pm 1$), $p_{oT} \to 0$ or ∞. Equation 110 can therefore be approximated as follows:

$$\left.\begin{aligned} e^{-2\theta_T} &\approx 1 - 4p_{oT} \; ; && p_{oT} \to 0 \\ e^{-2\theta_T} &\approx 1 - 4/p_{oT} ; && p_{oT} \to \infty \end{aligned}\right\} \tag{111}$$

Similarly, $z_o \to 0$ or ∞ at $x = \pm 1$, so that Eq. 103 becomes

$$\left.\begin{aligned} \rho^2 &\approx 1 - 4z_o \; ; && z_o \to 0 \\ \rho^2 &\approx 1 - 4/z_o ; && z_o \to \infty \end{aligned}\right\} \tag{112}$$

Substituting Eq. 111 and Eq. 112 in Eq. 108 yields the desired result:

$$\left[\begin{aligned} a_N &= \ln \left| 1 + \frac{p_{oT}}{z_o} \right| \; ; && z_o \to 0, \quad p_{oT} \to 0 \\ a_N &= \ln \left| 1 + \frac{1}{p_{oT} z_o} \right| ; && z_o \to 0, \quad p_{oT} \to \infty \\ a_N &= \ln \left| 1 + p_{oT} z_o \right| ; && z_o \to \infty, \quad p_{oT} \to 0 \\ a_N &= \ln \left| 1 + \frac{z_o}{p_{oT}} \right| \; ; && z_o \to \infty, \quad p_{oT} \to \infty \end{aligned}\right] \tag{113}$$

where the indicated magnitudes are evaluated at x = +1 or x = -1, depending on where the corresponding conditions on z_o and p_{oT} apply.

4.4 INCIDENTAL DISSIPATION

With the exception of filters having very narrow bandwidths, the effects of dissipation in crystal elements employed in filters may be neglected. This statement will be discussed later. It is necessary to show first that inductances, which are 100 times more dissipative than crystals, may be introduced into a crystal-filter network in such a manner that the essential advantages offered by the crystal elements are not lost.

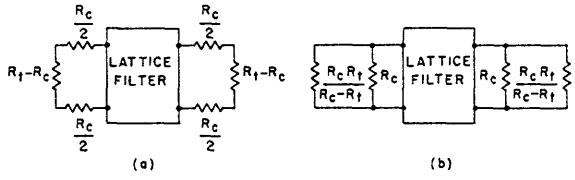

Fig. 23. Resistance-compensated networks.

Let us refer to filters 3 and 5 of Fig. 9. If the resistances associated with the series inductances L_o and L_o' are equal (or are made equal by adding resistance to the smaller one), then by the theorems illustrated in Fig. 8, these resistances may be removed from the lattice and placed in series with the filter network, as shown in Fig. 23a. Similar reasoning would bring the effective parallel resistance of shunt inductances (filter 4 of Fig. 9) outside of the lattice, as shown in Fig. 23b. The resistances brought out of the lattice may be incorporated in the terminal resistances of the filter and will add a constant loss to the insertion loss characteristic. Networks of this kind, in which the dissipation of lossy elements can be made to introduce a constant loss without affecting the filter selectivity, are called resistance-compensated networks (5).

The loss introduced by the effective resistance (R_c) of the inductances may be computed as follows. In the case of series inductances, taking $L_o = L_o'$, Eq. 94 yields

$$R_t = a_o R_o = a_o \, 2\pi f_o \, L_o \, B_r \tag{114}$$

From Fig. 23a, the insertion loss (a_c) introduced by R_c becomes

$$a_c = -20 \log \left(1 - \frac{R_c}{R_t}\right) \text{db} \tag{115}$$

The ratio of reactance to resistance (Q_c) for the inductance L_o, in the vicinity of the filter passband, is given by

$$Q_c = \frac{2\pi f_o \, L_o}{R_c} \tag{116}$$

Substituting Eq. 114 and Eq. 116 in Eq. 115 yields

$$a_c = -20 \log \left(1 - \frac{1}{a_o Q_c B_r}\right) \text{ db} \tag{117}$$

When two filters of the kind described above are cascaded to form a composite filter network, it is necessary to introduce resistance in series or in parallel at the common junction so that each filter will be properly terminated (28). The presence of these impedance-matching resistors adds an additional constant loss to the composite network.

From Eq. 117 it is apparent that a filter using series inductances can have a minimum bandwidth given by

$$B_{r(min)} = \frac{1}{a_o Q_c} \approx \frac{125}{Q_c} \text{ per cent (for } a_o \approx 0.8) \tag{118}$$

A similar result is obtained in the case of parallel inductances.

The range of bandwidths obtainable with filters employing quartz crystals and inductances extends, therefore, from below 1 per cent to about 13 per cent, and covers cases not practicable with crystals alone, or with conventional circuit elements.

The dissipation of the crystal elements in a crystal filter cannot be compensated in the manner described above. However, since Q's of 10,000 or greater are common for quartz resonators, the corresponding dissipation is extremely small. For this reason, it will be sufficient to determine the dissipative attenuation at several important points of the filter characteristic. Accordingly, the value of attenuation in the presence of dissipation ($\bar{a}$) will be determined at the filter center frequency (x=0), at the cutoff frequencies ($x = \pm 1$), and at the frequency of the attenuation peak ($x = x_\infty$). The method employed was suggested by E. A. Guillemin (21).

It is sufficient to compute $\bar{a}$ for a single basic section, since the dissipative attenuation for a filter equivalent to a number of cascaded basic sections will be the sum of the corresponding attenuations for each section, as long as all crystal resonators have approximately the same Q values. Use is made of the normalized expression for attenuation given by

$$a = \ln \left| \frac{1 + p_o}{1 - p_o} \right| \tag{119}$$

where

$$p_o = m\left(\frac{x+1}{x-1}\right)^{1/2} \tag{120}$$

and

$$m = \left(\frac{x_\infty - 1}{x_\infty + 1}\right)^{1/2} \tag{121}$$

The analysis of a dissipative network is based upon the conclusion (29) that the impedance or propagation function of a uniformly dissipative network may be obtained

from the corresponding quantity of the lossless network by replacing $j\omega$ by $j\omega + \epsilon$, where

$$\epsilon = \frac{1}{2}\left[\frac{R}{L} + \frac{G}{C}\right] \tag{122}$$

Since

$$x = \frac{f - f_o}{B/2} = \frac{\omega - \omega_o}{\pi B} \tag{123}$$

the value of p_o for the dissipative network ($\bar{p}_o$) is obtained from p_o for the lossless network by replacing jx by $(jx + \epsilon/\pi B)$. Furthermore, from Eq. 122

$$\frac{\epsilon}{\pi B} = \frac{\omega_o}{\pi B}\left[\frac{R}{L\omega_o} + \frac{G}{C\omega_o}\right] = \frac{1}{Q_o B_r} \tag{124}$$

In crystal filters Q_o is essentially the Q of the crystal element, since the capacitors employed in the network are usually small air trimmers and may be considered dissipationless. With the use of Eq. 124, it is possible to write

$$\bar{p}_o(x) = p_o\left(x + \frac{1}{jQ_o B_r}\right) \tag{125}$$

a. Center frequency

In the vicinity of the filter center frequency, $x \to 0$ and Eq. 120 can be approximated by

$$p_o \approx jm\left[1+x\right]; \qquad x \to 0 \tag{126}$$

By making use of Eq. 126, Eq. 125 becomes (at x = 0)

$$\bar{p}_o(0) = \frac{m}{Q_o B_r} + jm \tag{127}$$

Substitution of Eq. 117 in Eq. 119 and the use of $\ln\left[1+u\right] \approx u$ yields

$$\bar{\alpha}_{x=0} \approx \frac{2m}{1 + m^2}\left(\frac{1}{Q_o B_r}\right) \quad \text{nepers} \tag{128}$$

b. Cutoff frequencies

In the vicinity of the lower cutoff, $p_o \to 0$; in the vicinity of the upper cutoff, $p_o \to \infty$. If the real part of $\bar{p}_o$ is denoted by $R_e\bar{p}_o$, then

$$\left.\begin{aligned} \bar{\alpha} &= \ln\left|\frac{1+\bar{p}_o}{1-\bar{p}_o}\right| \approx 2R_e\,\bar{p}_o(-1); && x = -1 \\ \bar{\alpha} &= \ln\left|\frac{1+\frac{1}{\bar{p}_o}}{1-\frac{1}{\bar{p}_o}}\right| \approx 2R_e\,\frac{1}{\bar{p}_o(1)}\ ; && x = +1 \end{aligned}\right\} \tag{129}$$

Using Eq. 125 and Eq. 120, we have

$$\bar{p}_o(-1) \approx \frac{m}{(2)^{1/2}}\left[\frac{j}{Q_o B_r}\right]^{1/2} \tag{130}$$

$$\bar{p}_o(1) \approx m(2)^{1/2}\left[\frac{j}{Q_o B_r}\right]^{-1/2}$$

The desired result is obtained by taking the real parts of $\bar{p}_o(-1)$ and $\bar{p}_o(1)$ in Eq. 130, and by using Eq. 129.

$$\left.\begin{aligned} \bar{\alpha}_{x=-1} &\approx \frac{m}{(Q_o B_r)^{1/2}} \quad \text{nepers} \\ \bar{\alpha}_{x=+1} &\approx \frac{1}{m(Q_o B_r)^{1/2}} \quad \text{nepers} \end{aligned}\right\} \tag{131}$$

c. Attenuation peak

Near the attenuation peak, $p_o \to 1$, so that p_o can be approximated by

$$p_o \approx 1 + \left(\frac{dp_o}{dx}\right)_{x=x_\infty}(x - x_\infty); \qquad x \to x_\infty \tag{132}$$

On the other hand, if $\bar{p}_o$ in Eq. 125 is approximated by two terms of a Taylor series,

$$\bar{p}_o \approx p_o - j\left(\frac{dp_o}{dx}\right)\frac{1}{Q_o B_r} \tag{133}$$

Substituting Eq. 132 in Eq. 133 yields

$$\bar{p}_o \approx 1 + \left[(x - x_\infty) - j\frac{1}{Q_o B_r}\right]\left(\frac{dp_o}{dx}\right)_{x=x_\infty} \tag{134}$$

Taking the derivative indicated in Eq. 134 and using Eq. 119 and Eq. 121, we have

$$\bar{a} \approx \ln \frac{2\left(x_\infty^2 - 1\right) Q_o B_r}{\left[1 + Q_o^2 B_r^2 (x - x_\infty)^2\right]^{1/2}} \tag{135}$$

Equation 135 is the value of $\bar{a}$ in the vicinity of the attenuation peak. The maximum value of this expression occurs at $x = x_\infty$, and is given by

$$\bar{a}_{max} \approx \ln \left[2Q_o B_r \left(x_\infty^2 - 1\right)\right] \tag{136}$$

Equations 128, 131, and 136 make it possible to estimate the effect of using crystals with $Q = Q_o$ in any crystal filter of relative bandwidth B_r. Since $Q \geq 20,000$ in general, only filters with very small bandwidths or with peaks very close to the cutoff frequencies will be affected to any significant extent by crystal dissipation.

V. TOPICS PERTAINING TO THE REALIZATION OF CRYSTAL FILTERS

5.1 SPECIFICATION OF TOLERANCES ON CRYSTAL UNITS

Having successfully completed the synthesis of a particular filter, the designer is faced with the problem of determining the tolerances to which the element values must be held to ensure that the filter characteristics meet specifications. When the filter contains crystal elements, and is realized in lattice form, it becomes especially difficult to determine the tolerance. First of all, the lattice structure is a Wheatstone bridge and thus it is particularly sensitive to element variations. Moreover, the crystal units will ordinarily be supplied by the manufacturer in sealed enclosures with no provision for varying the parameters of the crystals. Fortunately, quartz resonators are stable and reliable circuit elements and are well suited for use in lattice structures. However, since there is no "variable" crystal in the same sense as a variable inductor or capacitor, the determination of tolerance limits by empirical means involves the costly procedure of grinding many crystals with slightly differing characteristics. By making use of the approximation techniques described in Section III a simple means of specifying tolerances analytically can be derived.

The alignment procedure normally employed for lattice filter (15) will adjust the values of C_o and C'_o of the filter network. The remaining quantities, which must be specified within certain limits, are the crystal resonant frequencies f_a and f'_a, the crystal capacitance C_1, the external inductances L_o, and the ratio C_1/C'_1. The resonant frequencies offer no difficulty, since the crystal manufacturer is accustomed to produce crystals for oscillator circuits, in which the required frequency tolerances are generally much more exact than in filter circuits. Normal frequency tolerances for filter crystals vary from ± 0.001 per cent to ± 0.02 per cent, depending on the filter bandwidth (30). Furthermore, so long as the ratio C_1/C'_1 remains constant, variations of C_1 can affect only the image impedance of narrow-band filters, or the shape of the passband in wideband filters. In the latter case, the effect may be estimated by varying L_o instead of C_1.

The remaining quantity, C_1/C'_1, is of primary importance in determining the attenuation characteristic of the filter. The procedure for calculating the permissible variation in this ratio will be as follows. The frequencies of peak attenuation ($f_{\infty 1}$ and $f_{\infty 2}$) will be determined in terms of C_1/C'_1, f_a, and f'_a. Keeping one peak fixed, which will be done in the alignment procedure, the permissible variation of the other peak is then found by making use of a set of normalized basic section characteristics (Fig. 12). The width of the passband is assumed to be constant, since, as a general

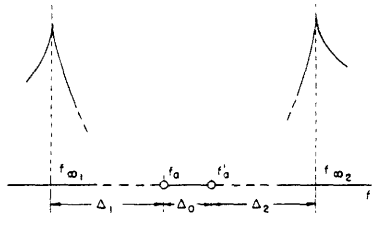

Fig. 24. Notation employed in sections 5.1 – 5.2.

rule, very small variations of C_1/C_1' are involved, and corresponding variations of filter bandwidth are even smaller. Finally, the permissible range of attenuation peak values is expressed as a tolerance limit on C_1/C_1'.

The first step of the procedure outlined above is accomplished by writing the condition for an attenuation peak in terms of the admittances of Z_a and Z_b. That is, since $Z_a = Z_b$ at $f = f_{\infty 1,2}$, then correspondingly,

$$Y_a = Y_b \tag{137}$$

where $Y_{a,b} = 1/Z_{a,b}$.

With the notation of Fig. 18 and Fig. 24, Eq. 137 may be written

$$j2\pi fC_o - j2\pi fC_1 \frac{f_a^2}{\left(f_{\infty 1,2}^2 - f_a^2\right)} = j2\pi fC_o' - j2\pi fC_1' \frac{(f_a')^2}{\left[f_{\infty 1,2}^2 - (f_a')^2\right]} \tag{138}$$

At each attenuation peak, Eq. 138 becomes

$$(C_o - C_o') = \frac{C_1 f_a^2}{f_{\infty 1}^2 - f_a^2} - \frac{C_1'(f_a')^2}{f_{\infty 1}^2 - (f_a')^2} \tag{139}$$

$$(C_o - C_o') = \frac{C_1 f_a^2}{f_{\infty 2}^2 - f_a^2} - \frac{C_1'(f_a')^2}{f_{\infty 2}^2 - (f_a')^2} \tag{139a}$$

Subtracting Eq. 139a from Eq. 139 and simplifying the result yields

$$\frac{C_1}{C_1'} = \frac{(f_a')^2}{f_a^2} \frac{\left(f_{\infty 1}^2 - f_a^2\right)\left(f_{\infty 2}^2 - f_a^2\right)}{\left[f_{\infty 1}^2 - (f_a')^2\right]\left[f_{\infty 2}^2 - (f_a')^2\right]} \tag{140}$$

Equation 140 may be put into a much simpler form by employing an approximation technique similar to the one described in Section III. The notation involved is shown in Fig. 24; Δ_1 and Δ_2 are positive when one peak lies on each side of the filter passband. That is,

$$\begin{aligned} \Delta_1 &\equiv f_a - f_{\infty 1} \\ \Delta_2 &\equiv f_{\infty 2} - f_a' \end{aligned} \tag{141}$$

Note that the extent of the passband is not specified, since Eq. 140 holds for narrow-band or wideband filters, so long as no inductances are contained within the lattice itself.

The approximate form of Eq. 140 is obtained by writing

$$\left.\begin{aligned} f_{\infty 1}^2 &= (f_a - \Delta_1)^2 = f_a^2 - 2\Delta_1 f_2 + \Delta_1^2 \\ f_{\infty 2}^2 &= (f'_a + \Delta_2)^2 = (f'_a)^2 + 2\Delta_2 f'_a + \Delta_2^2 \\ (f'_a)^2 &= (f_a + \Delta_o)^2 = f_a^2 + 2\Delta_o f_a + \Delta_o^2 \\ f_a^2 &= (f'_a - \Delta_o)^2 = (f'_a)^2 - 2\Delta_o f'_a + \Delta_o^2 \end{aligned}\right\} \tag{142}$$

Substituting Eq. 142 in Eq. 140 and simplifying gives

$$\frac{C_1}{C'_1} = \frac{(f'_a)^2}{f_a^2} \frac{\Delta_1}{\Delta_2} \frac{(\Delta_2 + \Delta_o)}{(\Delta_1 + \Delta_o)} \frac{\left[1 - \dfrac{\Delta_o}{2f'_a + \Delta_2}\right]}{\left[1 - \dfrac{\Delta_o}{2f_a + \Delta_1}\right]} \tag{143}$$

If, in the bracketed expressions in Eq. 143, Δ_2 and Δ_1 are neglected compared to $2f'_a$ and $2f_a$, respectively, then Eq. 143 becomes

$$\frac{C_1}{C'_1} \approx \frac{f'_a}{f_a} \cdot \frac{1 + \dfrac{\Delta_o}{\Delta_2}}{1 + \dfrac{\Delta_o}{\Delta_1}} \tag{144}$$

The error involved in this approximation is completely negligible for all practical purposes.

To illustrate the use of Eq. 144, consider a narrow-band filter with one crystal in each lattice arm, which is designed in accordance with the procedure outlined in Table I. The desired attenuation characteristic is shown by the solid line in Fig. 25. Assume that the specifications given for the filter are such that if $x_{\infty 1}$ is held constant at -10, then the filter characteristic can vary between the dotted and dot-dash curves in Fig. 25, which correspond to $x_{\infty 2} = 8$ and $x_{\infty 2} = 12$, respectively. Thus $x_{\infty 2}$ varies by ± 20 per cent, and the attenuation above the upper peak ($x \approx 20$) varies by about ± 10 per cent. The corresponding variation in C_1/C'_1 is easily calculated from Eq. 144 by recognizing that f_a corresponds to $x = -1$, and f'_a corresponds to $x = 0$ in the symmetrical narrow-band filter. The ratio f'_a/f_a is essentially unity for this filter; and for the solid curve in Fig. 25, since $x_{\infty 2} = 10$, then $\Delta_o = 1$, $\Delta_1 = 9$, $\Delta_2 = 10$ (in terms of x). Thus, from Eq. 143, $C_1/C'_1 = \underline{0.99}$, which must correspond, of course, to the value of C_1/C'_1 obtained at step 8 in Table I. Similarly, for $x_{\infty 2} = 8$ and $x_{\infty 2} = 12$, $C_1/C'_1 = \underline{1.0125}$ and $\underline{0.975}$, respectively. The permissible variation of C_1/C'_1 is therefore ± 1.88 per cent.

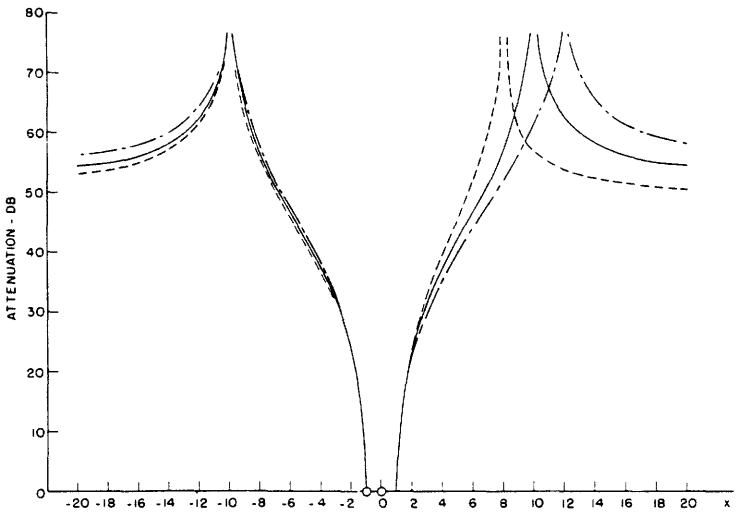

Fig. 25. Tolerance limits for narrow-band filter.

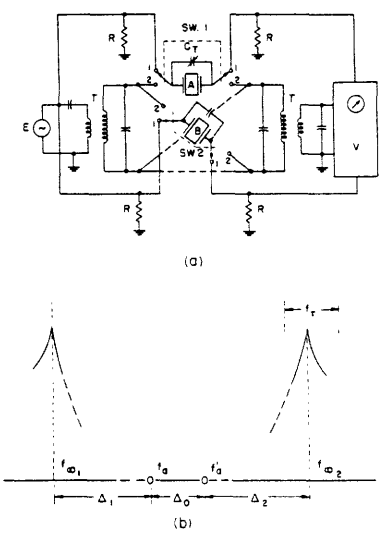

Fig. 26. Bridge method for adjustment of crystal units.

5.2 BRIDGE METHOD FOR ADJUSTMENT OF CRYSTAL UNITS

A number of methods commonly employed for the measurement of the equivalent electrical parameters of a crystal resonator are described in references 32 and 37 and will not be repeated here. However, a simple and accurate bridge method used by the author for adjusting the resonant frequencies and capacitance ratios (C_1/C_1') of crystal resonators used in filters will be discussed in some detail.

The measurement circuit is shown in Fig. 26a. With Sw.1 or Sw.2 in position 1, V will have a maximum indication when the oscillator E is tuned to the resonant frequency of crystal A(f_a) or crystal B(f_a'), respectively. The value of $\Delta_o = f_a' - f_a$ is measured or adjusted in this manner. With Sw.1 and Sw.2 both in position 2, crystals A and B are arranged in a lattice configuration of the type which would be employed for a narrow-band filter having one crystal in each lattice arm. Under these conditions the variable oscillator E is set to a frequency which is Δ_1 cycles below f_a, and the trimmer capacitors C_T (one in each series arm) are adjusted for minimum response at V. The oscillator frequency is then varied until the other attenuation peak ($f_{\infty 2}$ in Fig. 26b) is located. If the frequency difference between $f_{\infty 2}$ and f_a' is Δ_2, then the ratio C_1/C_1' (C_1 for crystal A, C_1' for crystal B) is given by Eq. 141 and Eq. 144:

$$\frac{C_1}{C_1'} = \frac{f_a'}{f_a} \cdot \frac{1 + \frac{\Delta_o}{\Delta_2}}{1 + \frac{\Delta_o}{\Delta_1}} \tag{145}$$

Nothing has been said thus far about optimum or reasonable values of Δ_o, Δ_1, and Δ_2. When Δ_o is less than the zero-pole spacing of a crystal, the measuring circuit is essentially a narrow-band filter and the attenuation peaks will be well defined. Furthermore, the impedance of the circuit will generally be in the region that will permit the coupling transformers T to be ordinary double-tuned coupled circuits (i-f transformers). If crystals A and B are to be used in a narrow-band filter, then f_a and f_a' can be the resonant frequencies called for in the filter design. On the other hand, the crystals may be employed in a wideband filter, in which case their resonant frequencies must be widely separated, and two alternatives are possible:

1. The frequency f_a is the resonant frequency of crystal A as called for by the filter design. Crystal B is adjusted to a frequency f_a', about 0.1 per cent of f_a (Δ_o) above f_a. The ratio C_1/C_1' is adjusted to

$$\frac{C_1}{C_1'} = \left(\frac{C_1}{C_1'}\right)_x \frac{f_a'}{(f_a')_x} \tag{146}$$

where $(C_1/C_1')_x$ and $(f_a')_x$ are the values called for in the filter design. When the resonant frequency of crystal B is subsequently raised to $(f_a')_x$ by decreasing the length of the resonator (a longitudinal vibration is assumed), then the capacitance of the crystal

will be decreased correspondingly, and the final ratio of series capacitances will be $(C_1/C_1')_x$.

2. Assume that two crystals have been ground and adjusted for use in a particular wideband filter, using the method described above. For other procedures the reader is referred to Article 6.1 of reference (38). Call these crystals A_s and B_s. When many such filters are needed, A_s and B_s must be duplicated a corresponding number of times. The bridge method is particularly suitable for this application, since A_s and B_s may then be used as "standards." Suppose, for example, that A_s has a resonant frequency of f_s. It is necessary, first, to regrind A_s to a frequency $f_s + \Delta_o$, where Δ_o is about 0.1 per cent of f_a. A_s, with frequency $f_s + \Delta_o$, is then placed in the "B" arm of the lattice (Fig. 26a). Any crystal may now be made identical to A_s by placing it in the "A" arm of the lattice and making the adjustments necessary to obtain

$$f_a = f_s$$

$$\frac{C_1}{C_1'} = 1$$

In a similar manner crystal B_s may serve as a standard from which any number of resonators are duplicated.

The choice of Δ_1 in Fig. 26b, that is, the location of $f_{\infty 1}$ relative to f_a, is based on a compromise between two considerations. On the one hand, an analysis of the measurement error, to be carried out presently, reveals that the accuracy of the bridge method increases as Δ_1 increases. On the other hand, if Δ_1 is made very large it will be difficult to distinguish the position of the attenuation peak, because of system noise. In general, a good compromise is achieved when Δ_1 is in the order of $10\Delta_o$.

The accuracy with which Δ_o, Δ_1, and Δ_2 must be measured is easily determined from Eq. 145. For example, if an error is made in the measurement of Δ_1, so that

$$\Delta_1^* = \Delta_1 + \epsilon_1 = \Delta_1 \left(1 + \frac{\epsilon_1}{\Delta_1}\right) \tag{147}$$

where

Δ_1^* = measured value of Δ_1 (cps)

Δ_1 = actual value of Δ_1 (cps)

ϵ_1 = error in measurement of Δ_1 (cps)

then the measured value of C_1/C_1', denoted by $(C_1/C_1')^*$, becomes, from Eq. 145

$$\left(\frac{C_1^*}{C_1'}\right) = \frac{f_a'}{f_a} \frac{1 + \frac{\Delta_o}{\Delta_2}}{1 + \frac{\Delta_o}{\Delta_1}\left(1 + \frac{\epsilon_1}{\Delta_1}\right)} \tag{148}$$

Assuming $\epsilon_1 << \Delta_1$, Eq. 148 may be written ·

$$\left(\frac{C_1^*}{C_1'}\right) = \frac{f_a'}{f_a} \cdot \frac{1 + \frac{\Delta_o}{\Delta_2}}{\left(1 + \frac{\Delta_o}{\Delta_1}\right)\left[1 - \frac{\epsilon_1}{\Delta_1}\left(\frac{\Delta_o}{\Delta_o + \Delta_1}\right)\right]} \tag{149}$$

Using Eq. 145, Eq. 149 is equivalent to

$$\left(\frac{C_1^*}{C_1'}\right) = \frac{C_1}{C_1'}\left[1 + \frac{\epsilon_1}{\Delta_1}\,\frac{1}{\left(\frac{\Delta_1}{\Delta_o} + 1\right)}\right] \tag{150}$$

That is, an error of ϵ_1 in Δ_1, corresponds to an error of

$$\frac{\epsilon_1}{\Delta_1\left(\frac{\Delta_1}{\Delta_o} + 1\right)}$$

in C_1/C_1'. If $\Delta_1 \approx 10\Delta_o$, then the percentage error in C_1/C_1' is less then one-tenth of the percentage error made in the measurement of Δ_1. A similar result is obtained for Δ_2.

When an error ϵ_o is made in the measurement of Δ_o, the effect upon C_1/C_1', is easily calculated from Eq. 145:

$$\left(\frac{C_1^*}{C_1'}\right) = \frac{C_1}{C_1'}\left[1 + \frac{\epsilon_o}{\Delta_o}\,\frac{\left(\frac{\Delta_2}{\Delta_o} - \frac{\Delta_1}{\Delta_o}\right)}{\left(\frac{\Delta_1}{\Delta_o} + 1\right)\left(\frac{\Delta_2}{\Delta_o} + 1\right)}\right] \tag{151}$$

The error in C_1/C_1', expressed by Eq. 151, can be made zero if $\Delta_1 = \Delta_2$. From Eq. 145, the condition $\Delta_1 = \Delta_2$ corresponds to

$$\frac{C_1}{C_1'} = \frac{f_a'}{f_a} = 1 + \frac{\Delta_o}{f_a} \approx 1 \tag{152}$$

since $f_a' = f_a + \Delta_o$ and $\Delta_o << f_a$.

From Eqs. 151 and 152, it is apparent that small deviations in the value of Δ_o resulting from measurement error or from tolerances placed on the resonant frequencies of the crystal units, will have negligible effects upon the accuracy of the bridge method if $\Delta_1 >> \Delta_o$, and if $C_1 \approx C_1'$. The latter condition is generally found to exist when crystals are designed for symmetrical narrow-band or wideband filters and when the bridge method is used to duplicate crystals.

As an example of the use of the bridge method, consider two resonators that must

satisfy the following requirements:

$$\left.\begin{aligned} f_a &= 100,000 \text{ cps} \\ f_a' &= 100,100 \text{ cps} \end{aligned}\right\} \tag{153}$$

$$\frac{C_1}{C_1'} = 1 \pm 0.01 \tag{154}$$

From Eq. 153: $\Delta_o = 100$ cps. The resonators are ground to yield the required resonant frequencies. As we explained previously, the bridge (Fig. 26a) is set to balance at $f_{\infty 1}$. In this case, taking $\Delta_1 = 10\Delta_o$, $f_{\infty 1} = 99,000$ cps. The crystal capacitances must now be adjusted, by removing the plating (34), until the attenuation peak $f_{\infty 2}$ lies within a range f_τ (Fig. 26b) determined by Eq. 154. From Eq. 145, we have

$$\frac{\Delta_o}{\Delta_2} = \frac{f_a}{f_a'}\frac{C_1}{C_1'}\left(1 + \frac{\Delta_o}{\Delta_1}\right) - 1 \approx 1.1\frac{C_1}{C_1'} - 1 \tag{155}$$

For $C_1/C_1' = 1 - 0.01$, and $C_1/C_1' = 1 + 0.01$, Eq. 155 yields

$$\Delta_2 = 8.9\Delta_o = 890 \text{ cps}$$

and

$$\Delta_2 = 11.1\Delta_o = 1110 \text{ cps}$$

respectively. The corresponding values of $f_{\infty 2}$ are 100,990 cps and 101,210 cps, respectively. The attenuation peak $f_{\infty 2}$ will therefore lie within the range $f_\tau = 220$ cps, for a deviation in C_1/C_1' of only ± 1 per cent. This result is not surprising, since the bridge method merely takes cognizance of the fact that the lattice is particularly sensitive to element variations. This fact, which creates a problem of considerable magnitude in connection with the realization of lattice filters, provides a corresponding advantage when element values must be accurately measured.

5.3 CONSTRUCTION OF CRYSTAL LATTICE FILTERS

Figure 27 shows the measured insertion loss characteristic of two narrow-band filters that were designed for use in a noise-spectrum analyzer (35). The center frequency is 80,000 cps, and the filter bandwidths are 10 cps and 100 cps, as indicated. Each filter is a single lattice section (filter 2, Fig. 9) employing two divided-plate crystals.

The equivalent electrical parameters of the resonators (fully plated) are approximately

$$\left.\begin{aligned} L_1 &= 39.7\ \text{h} \\ C_1 &= 0.1\ \mu\mu\text{f} \\ R_1 &= 900\ \Omega \\ C_o &= 17.0\ \mu\mu\text{f} \\ Q &= 22,000 \end{aligned}\right\} \tag{156}$$

Note: C_o includes crystal holder and socket capacitance. Referring to Fig. 27, the insertion loss shown for the 10-cycle filter is actually the combined loss of the 10-cycle and 100-cycle filters, since the two filters are connected in cascade when the analyzer is operated with 10-cycle bandwidth, thereby increasing slightly the over-all selectivity. An insertion loss of 6 db is introduced at the center frequency of the 10-cycle filter because of incidental dissipation in the crystal elements.

To determine the agreement that can be expected between the calculated and measured performances of a crystal-lattice filter, a narrow-band filter (B = 100 cps; f_o = 80 kc) and a wideband filter (B = 4 kc; f_o = 80 kc) were constructed with divided-plate crystals. The nominal values of the electrical parameters are listed in Eq. 156.

The narrow-band filter mentioned above was designed for the following characteristics:

$$\left.\begin{aligned} f_A &= 79,950\ \text{cps} & f_{\infty 1} &= 79,625\ \text{cps} \\ f_B &= 80,050\ \text{cps} & f_{\infty 2} &= 80,375\ \text{cps} \end{aligned}\right\} \tag{157}$$

correspondingly,

$$\left.\begin{aligned} B &= 100\ \text{cps} & x_{\infty 1} &= -7.5 \\ f_o &= 80,000\ \text{cps} & x_{\infty 2} &= +7.5 \end{aligned}\right\} \tag{158}$$

The total insertion loss (including reflection and interaction losses) is plotted in Fig. 28 (solid line).

The synthesis procedure outlined in Table I yields

$$\left.\begin{aligned} f_a &= 79,950 \\ f'_a &= 80,000 \\ C_1/C'_1 &= 0.982 \\ C_o/C'_o &= 0.982 \\ r &= r' = 800 \end{aligned}\right\} \tag{159}$$

The bridge method was used to make the necessary crystal adjustments.

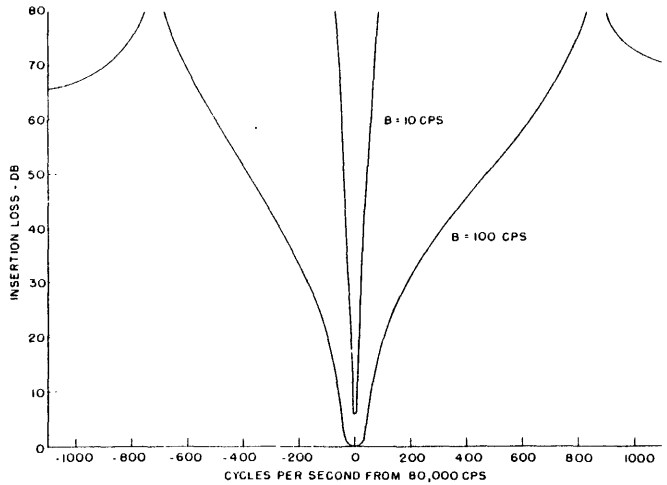

Fig. 27. Narrow-band filters for noise analyzer.

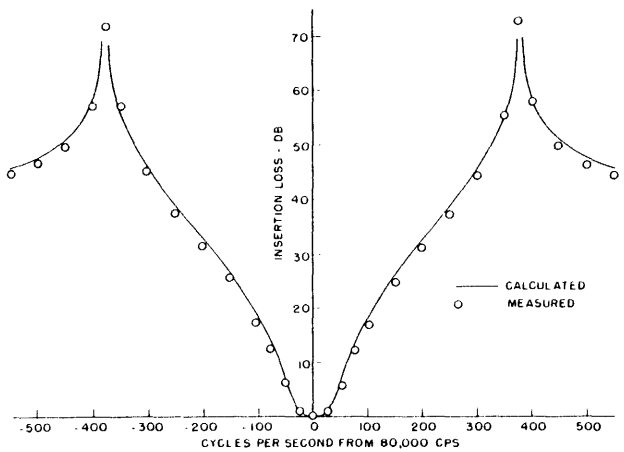

Fig. 28. Insertion loss characteristic of narrow-band filter.

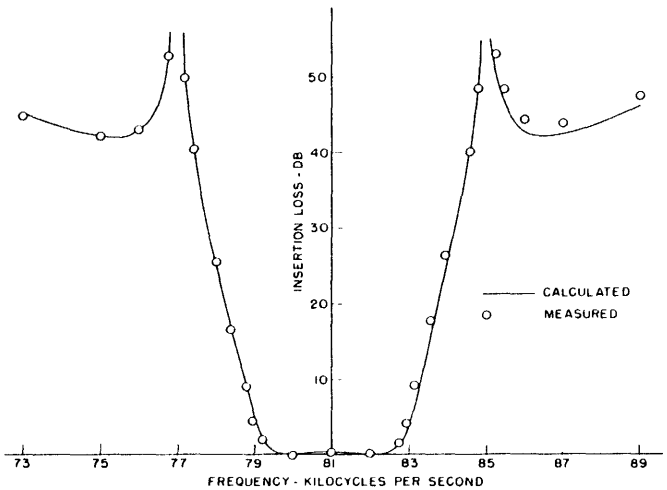

Fig. 29. Insertion loss characteristic of wideband filter.

Referring to Fig. 3a, which shows the divided-plate crystal connection employed in the filter, the impedance of the equivalent crystal in each lattice arm is seen to be twice the impedance of the corresponding fully plated crystal. Therefore, from Eq. 156:

$$\left.\begin{aligned} C_1 &= 0.05\ \mu\mu f \\ C_{ox} &= 8.5\ \mu\mu f \end{aligned}\right\} \tag{160}$$

The static capacitance of the crystal unit is denoted C_{ox} to distinguish it from the capacitance C_o called for by the design:

$$C_o = rC_1 = 40\ \mu\mu f \tag{161}$$

The shunt capacitance C_A (Fig. 3a) is therefore 40 - 8.5 = 31.5 $\mu\mu$f.

From Table III, the image impedance at f_o is:

$$R_o = \frac{1}{2\pi f_o C_o}\left(\frac{C_o}{C_o'}\right)^{1/2} \tag{162}$$

From Eqs. 158, 159, and 161:

$$R_o \approx 50,000\ \Omega \tag{163}$$

Double-tuned transformers, designed to yield a resistive impedance of 50 kilohms in the vicinity of the passband, were used to terminate the filter. The measured insertion loss at a number of frequencies is given in Fig. 28.

The final filter to be considered is a wideband filter having the following properties:

$$\left.\begin{aligned} f_A &= 79,000\ \text{cps} \\ f_B &= 83,000\ \text{cps} \\ f_{\infty 1} &= 77,000\ \text{cps} \\ f_{\infty 2} &= 85,000\ \text{cps} \\ f_{\infty 3} &= \infty \end{aligned}\right\} \tag{164}$$

The synthesis procedure outlined in Table II yields:

$$\left.\begin{aligned} f_a &= 79,885\ \text{cps} & C_o/C_o' &= 0.993 \\ f_a' &= 82,029\ \text{cps} & C_1/C_1' &= 1.014 \\ f_a &= 81,168\ \text{cps} & r &= 814.9 \end{aligned}\right\} \tag{165}$$

The filter was realized in the form shown in Fig. 10. Two divided-plate crystals that were adjusted by the bridge method to the required frequency and capacitance values were used. The value of the series inductance L_o is calculated as follows.

$$C_o = rC_1 = 814.9 \times 0.05 = 40.75\ \mu\mu f \tag{166}$$

From Eq. 58:

$$L_o = \frac{1}{4\pi^2 f_a^2 C_o} = 94.4\ \text{mh} \tag{167}$$

From Eq. 94, the image impedance at f_o is

$$R_o = 2\pi f_o L_o B_r \tag{168}$$

Since $B_r = B/f_o$, Eq. 168 becomes

$$R_o = 2\pi B L_o = 2370\ \Omega \tag{169}$$

The filter terminating resistance R_t was chosen to be $0.8\ R_o$, or 1900 ohms. The reflection and interaction losses corresponding to this termination ($a_o = 0.8$) are given by Fig. 22b. The total insertion loss for the filter is shown in Fig. 29, together with the measured loss at a number of frequencies. The insertion loss resulting from dissipation in the series inductances is approximately 6 db. This loss is not shown in Fig. 29, since the filter is resistance-compensated and the loss is the same at all frequencies.

The close agreement between calculated and measured filter characteristics in Figs. 28 and 29 justifies the time spent in determining the corresponding reflection and interaction losses. Because of the extremely low dissipation and the high stability of the quartz crystal, the designer may have a great deal of confidence in the fact that the filter that he has completed "on paper" will be realized in practice.

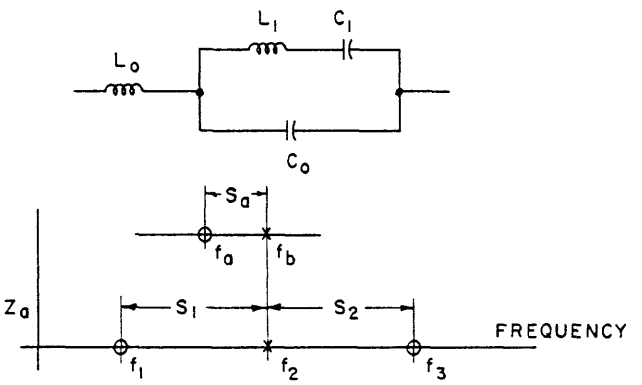

Fig. 30. Inductance in series with crystal.

APPENDIX I

ELEMENT VALUES OF FILTER REACTANCES

The calculations necessary for determining the element values of reactances used in crystal filters from the corresponding critical frequency configurations will now be described. The procedure involved is the same for all of the inductance-capacitance-crystal combinations listed in section 3.6. All element values are calculated in terms of the crystal shunt capacitance C_o (Fig. 15). A crystal unit is specified by its resonant frequency f_a, and its ratio of capacitances

$$r = \frac{C_o}{C_1} \tag{170}$$

The crystal series capacitance (C_1) and series inductance (L_1) are determined (in terms of C_o) if f_a and r are known. An inductance (L_o) placed in series or in parallel with a crystal is determined by the frequency at which it resonates C_o:

$$\omega_a \equiv 2\pi f_a \equiv \frac{1}{(L_o C_o)^{1/2}} \tag{171}$$

The exact solution for the reactance element values involves the determination of f_a, f_b, and f_∞ from the critical frequencies $f_1, f_2, \ldots$ (Fig. 14). The approximate solution is accomplished by determining the crystal zero-pole spacing (S_a) and the spacing between f_∞ and some fixed frequency, in terms of the critical frequency spacings $S_1, S_2, \ldots$ (Fig. 14).

To illustrate the method that can be used to determine the quantities mentioned above, the case of an inductance in series with a crystal will be discussed in detail. The notation involved is shown in Fig. 16, and is repeated in Fig. 30.

The reactance of the inductance is

$$Z_L = j2\pi f L_o \tag{172}$$

and the reactance of the crystal is given by

$$Z_c = \frac{-j}{2\pi f C_o} \cdot \frac{f^2 - f_a^2}{f^2 - f_b^2} \tag{173}$$

Combining Eqs. 172 and 173, using Eq. 171, and simplifying the result yields

$$Z_a = j2\pi f L_o \frac{\left(f^2 - f_1^2\right)\left(f^2 - f_3^2\right)}{f^2\left(f^2 - f_2^2\right)} \tag{174}$$

where

$$\left.\begin{aligned} f_2^2 &= f_b^2 \\ f_1^2 + f_3^2 &= f_b^2 + f_a^2 \\ f_1^2 f_3^2 &= f_a^2 f_a^2 \end{aligned}\right\} \tag{175}$$

Therefore, if f_1, f_2, and f_3 are specified, then from Eq. 175:

$$f_a = \left(f_1^2 + f_3^2 - f_2^2\right)^{1/2} \tag{176}$$

$$f_a = \frac{f_1 f_3}{f_a} \tag{176a}$$

$$f_b = f_2 \tag{176b}$$

The approximate solution is found by expressing every frequency in Eq. 175 in terms of its position relative to f_2. That is, from Fig. 30,

$$\frac{f_1^2}{f_2^2} = \frac{(f_2 - S_1)^2}{f_2^2} = 1 - \frac{2S_1}{f_2} + \frac{S_1^2}{f_2^2} \tag{177}$$

$$\frac{f_3^2}{f_2^2} = \frac{(f_2 + S_2)^2}{f_2^2} = 1 + \frac{2S_2}{f_2} + \frac{S_2^2}{f_2^2} \tag{178}$$

$$\frac{f_a^2}{f_2^2} = \frac{(f_2 - S_a)^2}{f_2^2} = 1 - \frac{2S_a}{f_2} + \frac{S_a^2}{f_2^2} \tag{179}$$

If a quantity Δ_a is defined by

$$\Delta_a \equiv f_a - f_2$$

then

$$\frac{f_a^2}{f_2^2} = \frac{(f_2 + \Delta_a)^2}{f_2^2} = 1 + \frac{2\Delta_a}{f_2} + \frac{\Delta_a^2}{f_2^2} \tag{180}$$

The approximate value of Δ_a is determined by writing Eq. 176 in the form:

$$\frac{f_a^2}{f_2^2} = \frac{f_1^2}{f_2^2} + \frac{f_3^2}{f_2^2} - 1 \tag{181}$$

Substituting Eqs. 177, 178, and 180 in Eq. 181 and neglecting terms containing $1/f_2^2$,

yields:

$$\left.\begin{aligned} 1 + \frac{2\Delta_a}{f_2} &\approx 1 + \frac{2S_2}{f_2} + 1 - \frac{2S_1}{f_2} - 1 \\ &= 1 + \frac{2(S_2 - S_1)}{f_2} \end{aligned}\right\} \tag{182}$$

or

$$\Delta_a \approx S_2 - S_1 \tag{183}$$

A first approximation for f_a is therefore given by

$$f_a \approx f_2 + (S_2 - S_1) \tag{184}$$

The crystal zero-pole spacing is determined from Eq. 176a and Eq. 181:

$$\frac{f_a^2}{f_2^2} = \frac{\frac{f_1^2}{f_2^2} \cdot \frac{f_3^2}{f_2^2}}{\frac{f_a^2}{f_2^2}} = \frac{\frac{f_1^2}{f_2^2} \cdot \frac{f_3^2}{f_2^2}}{\frac{f_1^2}{f_2^2} + \frac{f_3^2}{f_2^2} - 1} \tag{185}$$

Equations 177, 178, and 179 may now be substituted in Eq. 185. It is important to note, however, that although the last term in Eq. 179 may be neglected, the same is not true for Eq. 177 or Eq. 178. This is the result of the fact that S_a is very small compared to S_1 or S_2. There would be no justification for adding L_o to the crystal unit if this were not the case. Equation 185 may therefore be written in the form

$$1 - \frac{2S_a}{f_2} \approx \frac{\left(1 - \frac{2S_1}{f_2} + \frac{S_1^2}{f_2^2}\right)\left(1 + \frac{2S_2}{f_2} + \frac{S_2^2}{f_2^2}\right)}{1 + \frac{2(S_2 - S_1)}{f_2} + \frac{S_1^2 + S_2^2}{f_2^2}} \tag{186}$$

Expanding the numerator of the right side of Eq. 186 and neglecting terms containing $1/f_2^3$ and $1/f_2^4$, yields

$$\left.\begin{aligned} 1 - \frac{2S_a}{f_2} &\approx \frac{1 + \frac{2(S_2 - S_1)}{f_2} + \frac{S_1^2 + S_2^2}{f_2^2} - \frac{4S_1S_2}{f_2^2}}{1 + \frac{2(S_2 - S_1)}{f_2} + \frac{S_1^2 + S_2^2}{f_2^2}} \\ &= 1 - \frac{4S_1S_2}{f_2^2}\left[\frac{1}{1 + \frac{2(S_2 - S_1)}{f_2} + \frac{S_1^2 + S_2^2}{f_2^2}}\right] \end{aligned}\right\} \tag{187}$$

Approximating the bracketed expression in Eq. 187 by unity, a first approximation for S_a becomes

$$S_a \approx \frac{2S_1S_2}{f_2} \tag{188}$$

so that

$$f_a \approx f_2 - \frac{2S_1S_2}{f_2} \tag{189}$$

The ratio of capacitances, given by Eq. 170, may be calculated from f_a and f_b by Eq. 2:

$$r = \frac{f_a^2}{f_b^2 - f_a^2} \tag{190}$$

Or it may be approximated by noting that

$$\left.\begin{aligned} f_b^2 &= f_a^2 + 2S_af_a + S_a^2 \\ &\approx f_a^2 + 2S_af_a \end{aligned}\right\} \tag{191}$$

Substituting Eq. 191 in Eq. 190 yields

$$r \approx \frac{f_a}{2S_a} \tag{192}$$

In the case of an inductance in series with a crystal, Eq. 191 becomes

$$r \approx \frac{f_af_2}{2S_1S_2} \approx \frac{f_2^2}{2S_1S_2} \tag{193}$$

Acknowledgment

The author is indebted to Professor Henry J. Zimmermann for supervision and constant guidance, to Professors Jerome B. Wiesner, Ernst A. Guillemin, and Samuel J. Mason for many suggestions and helpful criticisms, and to Mr. Julian G. Ingersoll for skillful assistance in the fabrication and testing of the crystal filters and associated equipment.

References

1. R. A. Heising, Quartz Crystals for Electrical Circuits (D. Van Nostrand Company, Inc., New York, 1946) Chapter I.
2. W. G. Cady, The piezo-electric resonator, Proc. IRE, 10, 83 (April 1922).
3. K. S. Van Dyke, The piezo-electric resonator and its equivalent network, Proc. IRE, 16, 742 (June 1928).
4. W. P. Mason, Electric wave filters employing quartz crystals as elements, Bell System Tech. J., 13, 405-452 (July 1934).
5. W. P. Mason, Resistance-compensated band-pass crystal filters for unbalanced circuits, Bell System Tech. J., 16, 423-436 (Oct. 1937).
6. C. E. Lane, Crystal channel filters for the cable carrier system, Bell System Tech. J., 17, 125 (Jan. 1938).
7. J. P. Griffin and E. S. Pennell, Design and performance of EDT crystal units, Trans. AIEE, 67, 557-561 (1948).
8. W. P. Mason, Piezoelectric Crystals and Their Application to Ultrasonics (D. Van Nostrand Company, Inc., New York, 1950) Chapter IX.
9. W. G. Cady, Piezoelectricity (McGraw-Hill Book Company, New York, 1946) p. 297.
10. K. S. Van Dyke, A determination of some of the properties of piezo-electric quartz resonators, Proc. IRE, 23, 336 (April 1935).
11. R. A. Heising, op. cit., Chapter VI; XIV.
12. W. P. Mason, Low temperature coefficient quartz crystals, Bell System Tech. J., 19, 74-93 (Jan. 1940).
13. R. A. Heising, op. cit., Chapter XVII.
14. D. Indjoudjian and P. Andrieux, Les Filtres à Cristaux Piezoelectriques (Gauthiers-Villars, Paris, 1953) p. 47.
15. P. Vigoureux and C. F. Booth, Quartz Vibrators and Their Applications (His Majesty's Stationery Office, London, 1950) p. 286.
16. R. M. C. Greenidge, The mounting and fabrication of plated quartz crystal units, Bell System Tech. J., 23, 234 (July 1944).
17. W. P. Mason and R. A. Sykes, Electric wave filters employing quartz crystals with normal and divided electrodes, Bell System Tech. J., 19, 221-248 (April 1940).
18. E. A. Guillemin, Communication Networks (John Wiley and Sons, Inc., New York, 1935) Vol. II, Chapter X.
19. F. E. Terman, Radio Engineers' Handbook (McGraw-Hill Book Company, New York, 1943) p. 204.
20. R. M. Foster, A reactance theorem, Bell System Tech. J., 3, 259 (April 1924).
21. E. A. Guillemin, The effect of incidental dissipation in filters, Electronics, 19, 130-135 (Oct. 1946).
22. D. Indjoudjian and P. Andrieux, op. cit., p. 14.
23. W. P. Mason, Electromechanical Transducers and Wave Filters (D. Van Nostrand Company, Inc., New York, 1942) Chapter VIII.
24. W. Cauer, Siebschaltungen (VDI, Berlin, 1931).
25. P. Vigoureux and C. F. Booth, op. cit., Appendix 5.
26. E. A. Guillemin, Communication Networks, op. cit., pp. 303-306.

27. Ibid., pp. 295-297.

28. D. Indjoudjian and P. Andrieux, op. cit., pp. 84-85.

29. E. A. Guillemin, Communication Networks, op. cit., p. 445.

30. G. K. Burns, Manufacture of quartz crystal filters, Bell System Tech. J., 19, 516-532 (Oct. 1940).

31. D. Indjoudjian and P. Andrieux, op. cit., Chapter VIII; IX.

32. C. F. Booth, The application and use of quartz crystals in telecommunications, J. Inst. Elec. Engrs. (London), 88, pt. 3, 97-128 (June 1941).

33. W. G. Cady, Piezoelectricity, op. cit., p. 396.

34. E. S. Willis, A new crystal channel filter for broad band carrier systems, Trans. AIEE, 65, 134-138 (March 1946).

35. Quarterly Progress Report, Research Laboratory of Electronics, M.I.T., July 15, 1954, pp. 65-67.

36. B. O. Pierce, A Short Table of Integrals (Ginn and Company, Boston, 1929) p. 81.

37. E. A. Gerber, A review of methods for measuring the constants of piezoelectric vibrators, Proc. IRE, 41, 1103-1112 (Sept. 1953).

38. D. I. Kosowsky, The synthesis and realization of crystal filters, D. Sc. thesis, Department of Electrical Engineering, M.I.T., June 1955.